Dorsal horn interneuron-derived Netrin-4 contributes to spinal sensitization in chronic pain via Unc5B

Yasufumi Hayano,[1] Keiko Takasu,[2] Yoshihisa Koyama,[1] Moe Yamada,[1] Koichi Ogawa,[2] Kazuhisa Minami,[2] Toshiyuki Asaki,[2] Kazuhiro Kitada,[3] Satoshi Kuwabara,[4] and Toshihide Yamashita[1]

[1]Department of Molecular Neuroscience, Graduate School of Medicine, Osaka University, Suita, Osaka 565-0871, Japan
[2]Pain and Neuroscience, Discovery Research Laboratory for Core Therapeutic Areas, Shionogi & Co., Ltd., Toyonaka, Osaka 561-0825, Japan
[3]Department of Biological Sciences, Graduate School of Science, Hokkaido University, Kita-ku, Sapporo 060-0810, Japan
[4]Department of Neurology, Graduate School of Medicine, Chiba University, Chuo-ku, Chiba 260-8670, Japan

Because of the incomplete understanding of the molecular mechanisms that underlie chronic pain, the currently available treatments for this type of pain remain inefficient. In this study, we show that Netrin-4, a member of the axon guidance molecule family, was expressed in dorsal horn inner lamina II excitatory interneurons in the rat spinal cord. A similar expression pattern for Netrin-4 was also observed in human spinal cord. Behavioral analysis revealed that tactile and heat hyperalgesia after peripheral nerve injury or inflammation were abolished in Netrin-4–mutant rats. Transient suppression of Netrin-4 or its receptor Unc5B after injury could also prevent allodynia. Conversely, intrathecal administration of Netrin-4 protein to naive rats enhanced excitatory synaptic transmission in the dorsal horn and induced allodynia, suggesting that Netrin-4 is involved in spinal sensitization. Furthermore, the Unc5B receptor and subsequent activation of the tyrosine phosphatase SHP2 mediated Netrin-4–induced pain signaling in the spinal cord. These results identify Netrin-4 as a novel protein regulating spinal sensitization leading to chronic pain. Our findings provide evidence for the function of Netrin in the adult nervous system, as well as a previously unknown function in inducing pain signals from dorsal horn interneurons.

INTRODUCTION

Chronic pain, a debilitating syndrome that occurs after nerve damage or severe inflammation, can lead to hypersensitivity in the peripheral and central nervous systems (Woolf and Salter, 2000; Baron et al., 2010). Numerous studies have revealed that pain hypersensitivity, including tactile allodynia, results from aberrant excitability of dorsal horn neurons in the spinal cord evoked by peripheral sensory inputs (Costigan et al., 2009). Sensory information from primary afferents, which innervate the skin or deeper tissues, is processed by the excitatory or inhibitory interneurons of the dorsal horn and transmitted to the brain (Todd, 2010). Injury- or inflammation-induced alterations in the cellular properties of the dorsal horn circuit, such as enhanced synaptic transmission, increased membrane excitability, or reduced release or activity of γ-aminobutyric acid (GABA) and glycine, contribute to the development and maintenance of chronic pain (Latremoliere and Woolf, 2009). Therefore, the elucidation of the molecular mechanisms that underlie hyperexcitability in the dorsal horn could be important for developing more effective pain-relief treatment regimens (Baron, 2006). Previous studies have identified several pain-inducing factors that are derived from the axon terminals of primary afferents, activated glial cells, and immune cells (Latremoliere and Woolf, 2009). However, few pain-inducing molecules from dorsal horn interneurons have been identified.

Netrin, a laminin-related extracellular protein, was originally identified as an attractant molecule for axon guidance in the embryonic spinal cord (Kennedy et al., 1994; Cirulli and Yebra, 2007). In mammals, four secreted types (Netrin-1, -3, -4, and -5) and two glycosylphosphatidylinositol-anchored types (Netrin-G1 and -G2) have been identified (Koch et al., 2000; Nakashiba et al., 2000; Cirulli and Yebra, 2007). Secreted Netrins bind to DCC (deleted in colorectal cancer), Neogenin, and Unc5 homologue family members, whereas Netrin-Gs bind to different proteins (Sun et al., 2011). Previous findings have also shown that Netrin has important roles in cell migration, survival, axon branching, and synaptogenesis during neural development (Schwarting et al., 2004; Manitt et al., 2009; Takemoto et al., 2011; Hayano et al., 2014). Recent studies have reported that abnormal expression of either Netrin or its receptors leads to impairments in neural circuitry and neurodegenerative diseases in humans (Maraganore et al., 2005; Lesnick et al., 2007; Srour et al., 2010). However, the functional role of Netrin in the adult central nervous system remains poorly understood.

Correspondence to Toshihide Yamashita: yamashita@molneu.med.osaka-u.ac.jp

Abbreviations used: CSF, cerebrospinal fluid; DCC, deleted in colorectal cancer; DRG, dorsal root ganglia; eEPSC, evoked EPSC; EPSC, excitatory postsynaptic current; GABA, γ-aminobutyric acid; GFAP, glial fibrillary acidic protein; IB4, isolectin B4; I-O, input-output; lamina IIi, inner lamina II; lamina IIo, outer lamina II; PB, phosphate buffer; PSL, partial sciatic nerve ligation; RT, room temperature; sEPSC, spontaneous EPSC; SOM, somatostatin; TBS, Tris-buffered saline; TBST, TBS/0.1% Tween 20.

The Rockefeller University Press $30.00
J. Exp. Med. 2016 Vol. 213 No. 13 2949–2966
https://doi.org/10.1084/jem.20160877

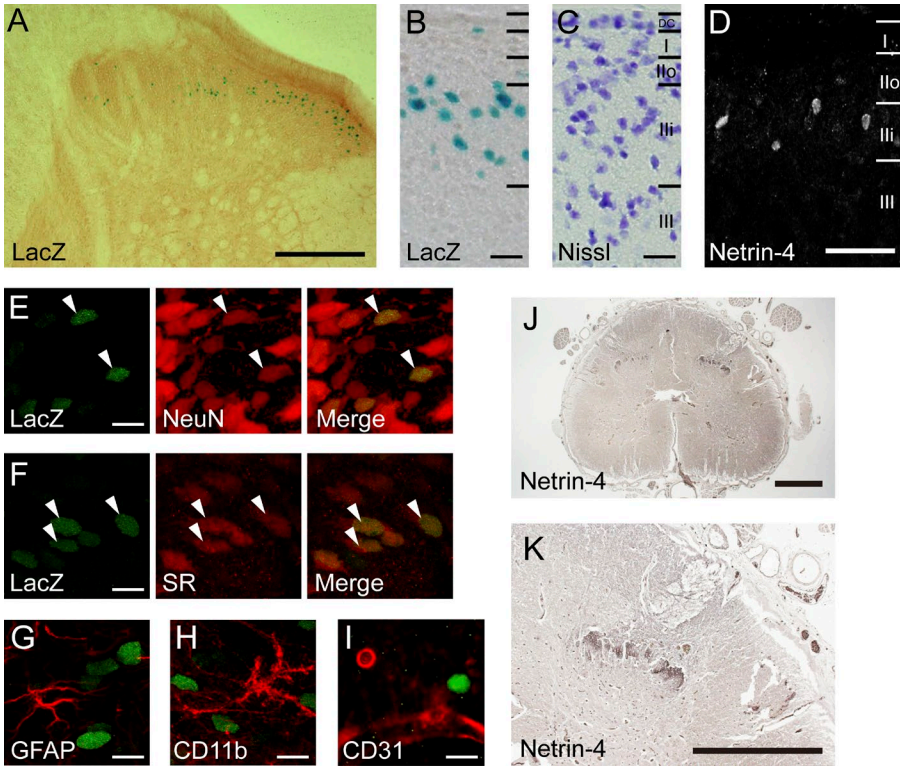

Figure 1. **Expression of Netrin-4 in the adult rat and human spinal cord.** (A) Spinal cord sections from heterozygous (*Tp/+*) rats showing LacZ$^+$ cells (blue). (B and C) Higher magnification of the dorsal horn (B) and adjacent Nissl-stained sections (blue; C). DC, dorsal column. (D) Netrin-4 immunohistochemistry in the superficial dorsal horn. (E–I) Coimmunostaining with cell type–specific markers (red): NeuN (E), serine racemase (SR; F), GFAP (G), CD11b (H), and CD31 (I). Arrowheads indicate colocalization of LacZ and markers. (J) Netrin-4 immunohistochemistry in human lumbar cord sections from individuals with multiple sclerosis. (K) Higher magnification image of J. Bars: (A) 0.2 mm; (B, C, and E–I) 10 µm; (D) 0.1 mm; (J and K) 0.5 mm. Each experiment was performed twice.

The current study investigated the role of Netrin-4 in the adult spinal cord. We found that Netrin-4 is expressed in inner lamina II (lamina IIi) neurons of the dorsal horn and plays a role in enhancing mechanical and thermal sensitivity during neuropathic or inflammatory pain. Importantly, suppression of Netrin-4 or its receptor, Unc5B, attenuated allodynia after nerve injury or inflammation. In contrast to previous studies that observed the role of Netrin in axon guidance during embryonic stages (Kennedy et al., 1994; Cirulli and Yebra, 2007), our data indicate that Netrin acts as a pain-inducing molecule and is secreted from dorsal horn interneurons in the adult spinal cord.

RESULTS

Netrin-4 is expressed in excitatory interneurons in lamina IIi of the dorsal horn

The expression pattern of Netrin-4 in the adult spinal cord was analyzed using mutant rats in which the polyA-IRES-lacZ (β-galactosidase) sequence was inserted between exons 2 and 3 of the Netrin-4 gene using the Sleeping Beauty Transposase (Kitada et al., 2007). LacZ histochemical staining of spinal cord sections from heterozygotes (*Tp/+*) showed that Netrin-4 expression was exclusively localized to the dorsal horn (Fig. 1 A). A comparison with an adjacent Nissl-stained section suggested that the LacZ-positive (LacZ$^+$) cells were located in lamina IIi (Fig. 1, B and C).

Consistent with this observation, immunohistochemistry against Netrin-4 revealed that Netrin-4–expressing cells were specifically distributed in lamina IIi (Fig. 1 D). We used molecular markers to identify the type of Netrin-expressing cells and found that LacZ$^+$ cells in the rat spinal cord expressed the neuronal cell marker NeuN (Fig. 1 E) but not the astrocytic marker glial fibrillary acidic protein (GFAP; Fig. 1 G), microglial marker CD11b (Fig. 1 H), or endothelial marker CD31 (Fig. 1 I). This result indicates that Netrin-4 is expressed in lamina IIi neurons, the majority of which are interneurons that modulate and transmit sensory information from primary afferents (Yasaka et al., 2010). Furthermore, the LacZ$^+$ nuclei were colocalized with excitatory neuron markers serine racemase (Fig. 1 F; Tabata-Imai et al., 2014) and vGluT2 (Fig. S1 C). However, there was no overlap with the inhibitory neuron marker Pax2 (Cheng et al., 2004) or parvalbumin (Fig. S1, A–C; Antal et al., 1991). This finding implies that excitatory interneurons specifically express Netrin-4 (Todd, 2010). As a recent study reported that somatostatin (SOM)-expressing spinal excitatory neurons were crucial for transmitting mechanical pain (Duan et al., 2014), we assessed the colocalization of SOM and Netrin-4 in the dorsal horn. LacZ$^+$ nuclei were observed in SOM-expressing cells, although we also found a LacZ signal in SOM-negative cells (Fig. S1 D). This finding suggests that Netrin-4–expressing cells constitute a subpopulation of dorsal horn excitatory interneurons.

We also examined Netrin-4 expression in spinal cord sections from autopsies of individuals with multiple sclerosis because these individuals are known to have neuropathic pain (Fig. 1, J and K; Khan and Smith, 2014). In the human lumbar cord, Netrin-4 immunoreactivity was observed in the dorsal

horn in a lamina-specific fashion, similar to the rat (Fig. 1, A and K). This result suggests that dorsal horn–specific Netrin-4 expression is evolutionarily conserved between rodents and humans. We further assessed the innervation of primary afferents into Netrin-4–expressing cells in the dorsal horn. $LacZ^+$ cells were intermingled with isolectin B4 (IB4) staining, a marker of nonpeptidergic C fibers projecting to lamina IIi (Fig. S1, E and E'). In contrast, calcitonin gene-related peptide staining, a marker of peptidergic C fibers that primarily projects to lamina I and outer lamina II (lamina IIo), did not overlap with the $LacZ^+$ nuclei (Fig. S1, F and F′). vGluT1 staining to detect myelinated A fibers partially overlapped with $LacZ^+$ nuclei (Fig. S1, G and G′). Therefore, these results support the notion that Netrin-4 is secreted from excitatory interneurons in lamina IIi that modulate or transmit incoming sensory information from nonpeptidergic C fibers and a portion of A fibers.

Abolishment of tactile allodynia and heat hyperalgesia in Netrin-4 mutants after nerve injury

Nerve damage frequently alters the function of dorsal horn interneurons and can cause decreases in GABA/glycine release or increased excitatory transmission, leading to hyperexcitability in the dorsal horn (Todd, 2010). The localization of Netrin-4–expressing neurons in lamina IIi prompted us to hypothesize that Netrin-4 is involved in nociception and pathological pain after nerve injury or inflammation. To address this issue, the pain-related behavior of Netrin-4–mutant homozygotes (*Tp/Tp*), which express a truncated Netrin-4 protein, was examined (Fig. 2, A–C; Kitada et al., 2007). Our previous study showed that *Tp/Tp* rats lack Netrin-4 function (Hayano et al., 2014). We found that partial sciatic nerve ligation (PSL; Seltzer model; Seltzer et al., 1990) in wild-type (*+/+*; $n = 13$) littermates resulted in a decrease in the withdrawal threshold induced by tactile allodynia (Fig. 2 A; 2 d after injury, $P < 0.05$; 4, 7, 14, 21, and 28 d after injury, $P < 0.01$; Chaplan et al., 1994). However, we did not observe alterations in the withdrawal threshold of *Tp/Tp* rats ($n = 10$) in the side ipsilateral to the injury compared with the thresholds observed in the side contralateral to the injury (Fig. 2 B). Moreover, the changes in the relative threshold among the *Tp/Tp* rats were smaller than those in *+/+* rats (Fig. 2 C; 2, 4, and 28 d after injury, $P < 0.05$; 7, 14, and 21 d after injury, $P < 0.01$). We also examined the thermal sensitivity of the Netrin-4 mutants after nerve injury using the plantar test (Fig. 2, D–F; Hargreaves et al., 1988). After injury, the +/+ rats ($n = 6$) showed a decreased paw withdrawal latency in the side ipsilateral to the injury (Fig. 2 D; $P < 0.01$); in contrast, the *Tp/Tp* ($n = 7$) rats showed no significant difference in the latencies between the ipsilateral and contralateral sides (Fig. 2 E) and smaller changes in the relative latencies compared with the +/+ rats (Fig. 2 F; 14, 21, and 28 d after injury, $P < 0.05$; 7 d after injury, $P < 0.01$). Thus, these results showed that tactile allodynia and heat hyperalgesia were not induced in Netrin-4 mutants after nerve injury.

Transient suppression of Netrin-4 ameliorates neuropathic pain after nerve injury

Although there was no obvious alteration in the sensory inputs in *Tp/Tp* rats (Fig. S2, A and B), the fact that the *Tp/Tp* rats showed larger withdrawal thresholds compared with the *+/+* rats in the absence of injury raised the possibility that the attenuation of allodynia in the *Tp/Tp* rats resulted from a developmental defect (Fig. 2, B and E). Moreover, it is also possible that Netrin-4 expressed outside of the spinal cord, such as in the skin or cortex, contributes to pain perception (Hayano et al., 2014), although $LacZ^+$ cells were not observed in the dorsal root ganglia (DRG), in Schwann cells of the sciatic nerve, or in pain-related nuclei of the thalamus (Fig. S2, C–E). Therefore, it was necessary to specifically manipulate Netrin-4 expression in the spinal cord to analyze its function in lamina IIi.

We performed intraspinal suppression of Netrin-4 expression using double-stranded siRNA and an antibody (Fig. 2, G–I; Takahashi et al., 2010) to determine whether transient suppression of Netrin-4 in the spinal cord was sufficient for attenuating allodynia. The siRNAs directed against Netrin-4 (Netrin-4 siRNA) were intrathecally administered 7 d after injury. Fluorescent dye–conjugated siRNAs were observed in dorsal horn neurons in the lumbar cord (Fig. 2 G), but no fluorescence was observed in the thoracic cord or cerebral cortex (not depicted). *Netrin-4* mRNA expression in the spinal cord was significantly decreased at 2 d after intrathecal administration (Fig. 2 H), and mechanical sensitivity was measured (Fig. 2 I). After Netrin-4 siRNA administration ($n = 9$), the reduction in paw withdrawal thresholds was significantly recovered (Fig. 2 I; 9 d after injury, $P < 0.05$; 10 and 11 d after injury, $P < 0.01$ vs. the control siRNA-treated group). Thus, the transient suppression of Netrin-4 expression in the spinal cord was sufficient for attenuating tactile allodynia in neuropathic pain.

Suppression of Netrin-4 attenuates allodynia in a model of inflammatory pain

We also examined whether deletion of the Netrin-4 gene affected allodynia in a model of inflammatory pain (Fig. 3). Subcutaneous injection of CFA into the hind paw induced tactile allodynia in +/+ rats (Fig. 3 A; Newbould, 1963). In contrast, *Tp/Tp* rats did not show a significant decrease in the withdrawal threshold (Fig. 3 B), suggesting that inflammatory pain was not induced. There were also significant differences in the relative changes in the threshold of the *Tp/Tp* rats after inflammation compared with the +/+ rats (Fig. 3 C; 1, 2, 4, and 7 d after CFA injection, $P < 0.01$). Moreover, intrathecal injection of Netrin-4 siRNA 4 d after the CFA injection significantly reversed the withdrawal threshold of the ipsilateral hind paw (Fig. 3 D; 7 d after CFA injection, $P < 0.05$; 6 and 8 d after CFA injection, $P < 0.01$ vs. the control siRNA-treated group). These observations indicated that suppression of Netrin-4 expression effectively attenuated both inflammatory and neuropathic pain.

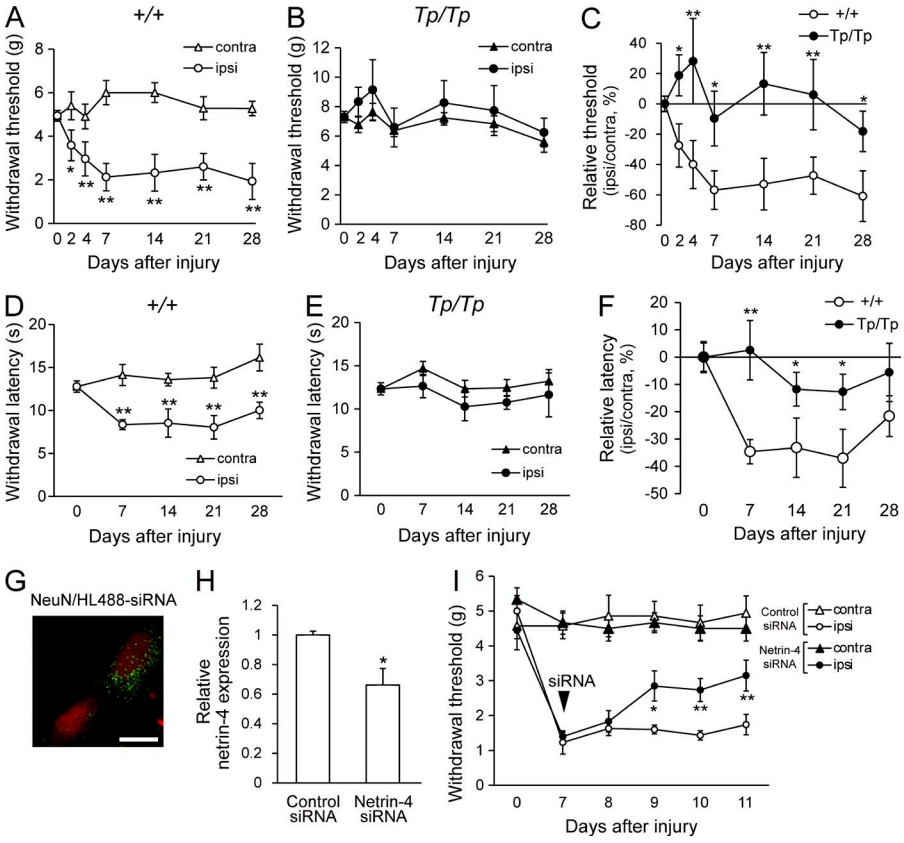

Figure 2. **Suppression of Netrin-4 expression attenuates tactile allodynia in neuropathic pain.** (A and B) Paw withdrawal thresholds of Netrin-4–mutant homozygotes (*Tp/Tp*; $n = 10$; A) and wild-type littermates (*+/+*; $n = 13$; B) to mechanical stimulation after PSL injury. (C) Relative withdrawal thresholds. (D and E) Post-injury withdrawal latencies of *+/+* (open; $n = 6$; D) and *Tp/Tp* (closed; $n = 7$; E) animals to thermal stimuli. (F) Relative withdrawal latency. (G) Localization of a fluorescent dye–conjugated siRNA (HiLyte-488; green) and NeuN immunofluorescence (red) in the dorsal horn of the spinal cord at 2 d after intrathecal administration. Bar, 10 µm. (H) Netrin-4 mRNA expression in the spinal cord at 2 d after siRNA administration. (I) Paw withdrawal thresholds of control siRNA (closed; $n = 9$)– or Netrin-4 siRNA (open; $n = 10$)–treated animals after PSL injury. The data are presented as the mean ± SEM. *, $P < 0.05$; **, $P < 0.01$; Tukey-Kramer test. Each experiment was performed three times. contra, contralateral; ipsi, ipsilateral.

Netrin-4 induces hyperexcitation in dorsal horn neurons and tactile allodynia

Recombinant Netrin-4 protein was intrathecally administered via a catheter implanted in the lumbar subarachnoid space of naive rats and an osmotic pump to determine whether the expression of Netrin-4 in the spinal cord was sufficient to induce hyperalgesia (Fig. 4; Maeda et al., 2009). The paw withdrawal thresholds to mechanical stimuli were then assessed at 12, 24, and 48 h after administration (Fig. 4 A). Continuous administration of Netrin-4 (200 ng/d; $n = 11$) or administration of 10% Netrin-4 (20 ng/d; $n = 6$) markedly decreased the paw withdrawal thresholds (Fig. 4 B; $P < 0.01$ vs. saline at 24 h after administration), whereas saline ($n = 12$), 1% Netrin-4 (2 ng/d; $n = 3$), or heat-denatured Netrin-4 ($n = 3$) had no effect on the paw withdrawal thresholds (Fig. 4, A and B). Cellular alterations in dorsal horn neurons resulting from Netrin-4 administration were examined with an immunohistochemical analysis of c-fos, a marker of neuronal activation (Fig. 4 C). The number of c-fos$^+$ cells was increased in the Netrin-4–treated spinal cords (right) compared with the saline-treated group (left; Fig. 4 D; $P < 0.01$; $n = 4$ for each group). Netrin-4 treatment significantly increased the number of c-fos$^+$ cells in lamina IIo, IIi, and III (Fig. 4 E; $P < 0.01$; $n = 4$ for each group). To further characterize c-fos$^+$ cells induced by Netrin-4, low-intensity mechanical stimulation was applied to the unilateral hind paw by paintbrush after Netrin-4 administration. Brushing after Netrin-4 administration increased the number of c-fos$^+$ cells in the dorsal horn, compared with the contralateral side (Fig. 4 F; $P < 0.001$; $n = 7$) or saline-treated group ($P < 0.01$; $n = 3$), indicating that Netrin-4 increases stimuli-evoked excitability in the spinal cord.

Numerous studies have revealed that glial activation induced by peripheral nerve injury or inflammation contributes to the development and maintenance of neuropathic pain (Tsuda et al., 2003; Ji et al., 2013). Thus, we also investigated whether microglia and/or astrocytes were activated by Netrin-4 administration by immunohistochemistry (Fig. 4, G and H). However, there was no obvious change in the number or morphology of Iba1$^+$ microglia (Fig. 4 G) or GFAP$^+$ astrocytes (Fig. 4 H) in the Netrin-4–treated spinal cords. After Netrin-4 treatment, the paw withdrawal threshold to mechanical stimuli was measured in the presence of glial inhibitors to further examine whether glial activation was involved in Netrin-4–induced allodynia (Fig. 4, I and J). Neither the microglial inhibitor minocycline ($n = 6$) nor the astrocyte inhibitor L-a-aminoadipate ($n = 4$) blocked the previously observed decrease in the paw withdrawal thresholds after Netrin-4 administration (Fig. 4, I and J). These results suggest that glial activation was not involved in Netrin-4–induced allodynia and that Netrin-4 directly increased the excitability of dorsal horn neurons, leading to tactile allodynia in neuropathic pain.

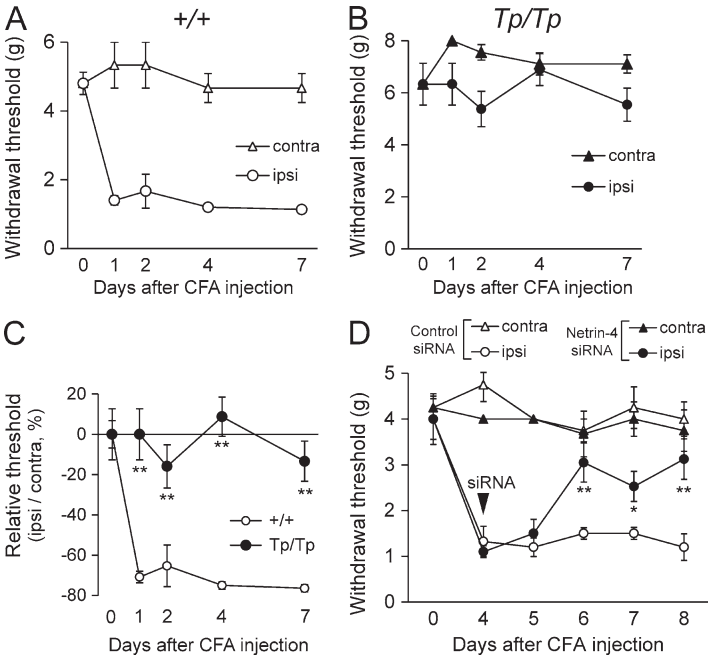

Figure 3. **Tactile allodynia in a model of inflammatory pain is prevented by suppressing Netrin-4.** (A and B) Paw withdrawal threshold of wild-type littermates (*+/+*; $n = 6$; A) and Netrin-4–mutant (*Tp/Tp*; $n = 6$; B) rats after CFA injections. After surgery, the *+/+* rats showed decreases in the thresholds on the ipsilateral (ipsi) side (A), whereas the *Tp/Tp* rats did not exhibit decreases (B). contra, contralateral. (C) Comparison of the relative withdrawal thresholds between *+/+* and *Tp/Tp* animals after CFA injections. (D) Effect of Netrin-4 siRNA on inflammation-induced tactile allodynia. The paw withdrawal threshold of the Netrin-4 siRNA–treated group (●; $n = 6$) was significantly increased compared with the control siRNA–treated group (○; $n = 6$). The data are presented as the mean ± SEM. *, $P < 0.05$; **, $P < 0.01$; Tukey-Kramer test. Each experiment was performed three times.

Netrin-4 enhances excitatory synaptic transmission in the dorsal horn

We next examined the electrophysiological changes in synaptic transmission in the dorsal horn using whole-cell patch recordings to further delineate how Netrin-4 promoted neuronal activation in the spinal cord and tactile allodynia (Fig. 5, A–G). At 24–48 h after Netrin-4 administration (Fig. S3), we generated lumbar spinal cord sections and recorded the excitatory postsynaptic currents (EPSCs) from lamina II neurons. Compared with the saline-treated rats, the frequency and amplitude of the spontaneous EPSCs (sEPSCs) were significantly increased in Netrin-4–treated rats (Fig. 5, A–C; $P < 0.01$; $n = 23$ for each group). Evoked EPSCs (eEPSCs) were recorded by stimulating neighboring areas to examine the synaptic responses of the dorsal horn neurons (Fig. 5, D and E). The input-output (I-O) relationship was investigated by measuring the eEPSC amplitude as a function of the afferent stimulus intensity (Cui et al., 2012). The I-O relation curve of the Netrin-4–treated spinal cords exhibited a leftward shift compared with the saline-treated groups (Fig. 5 E; $P < 0.0001$; $n = 23$ for each group). At stimulus intensities of 7, 10, and 15 V, the synaptic responses in Netrin-4–treated spinal cords were significantly larger than those in the saline-treated groups (Fig. 5 E; $P < 0.01$; $n = 23$ for each group). These results indicate that the evoked synaptic response in the dorsal horn was significantly enhanced by Netrin-4 administration.

Furthermore, the NMDA/non-NMDA ratio of the eEPSCs was studied by recording non–NMDA-type glutamate receptor (non-NMDAR)–mediated eEPSCs at −60 mV and NMDAR-mediated eEPSCs at 60 mV to further examine the synaptic properties of evoked responses of the dorsal horn neurons (Fig. 5 F; Iwata et al., 2007). In the Netrin-4–treated spinal cords, the NMDA/non-NMDA ratio was significantly increased compared with the saline-treated group, suggesting an increase in the NMDAR-mediated currents (Fig. 5 G; $P < 0.01$; $n = 23$ for each group). These electrophysiological analyses showed that Netrin-4 enhanced both spontaneous and evoked synaptic transmission in dorsal horn neurons. Consistent with these results, previous studies revealed that synaptic modulation, including increased NMD AR-mediated currents in the dorsal horn circuit, contributes to neuropathic or inflammatory pain (Guo and Huang, 2001; Petrenko et al., 2003; Iwata et al., 2007; Yanagisawa et al., 2010; Cui et al., 2012).

It is also known that phosphorylation of the NR2B subunit of NMDAR increases the open probability of NMD AR leading to neuronal activation (Kennedy and Manzerra, 2001). Indeed, a Western blot analysis of the spinal cord tissue revealed that Netrin-4 administration increased the level of phosphorylated NR2B compared with the saline-treated group but did not change the total NR2B expression level (Fig. 5, H–J; $P < 0.01$ vs. the saline group). This finding fits with electrophysiological results showing that the NMDAR-mediated currents were increased after Netrin-4 administration. Collectively, these results suggest that Netrin-4 enhanced synaptic transmission by modulating NMDAR in the dorsal horn.

Excitatory synaptic transmission in the dorsal horn is enhanced after peripheral nerve injury, and this enhancement is abolished with a Netrin-4 antibody

A Netrin-4 antibody was intrathecally injected into the spinal cord to investigate whether endogenous Netrin-4 was involved in the spinal synaptic mechanisms in the neuropathic

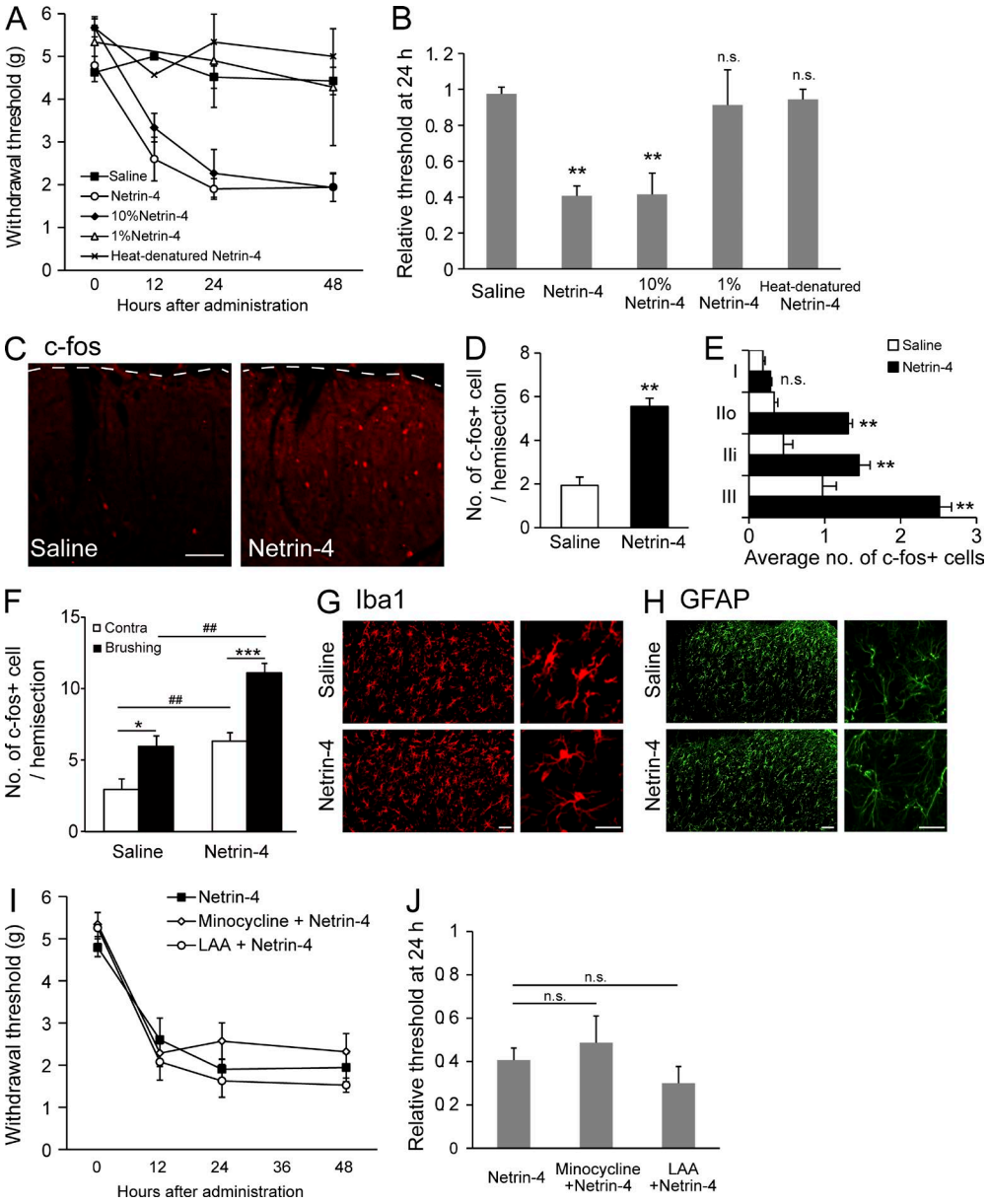

Figure 4. **Intrathecal administration of Netrin-4 induces tactile allodynia and neuronal activation.** (A) Paw withdrawal thresholds after naive rats were treated with Netrin-4 (200 ng/d; ○; $n = 11$), 10% Netrin-4 (20 ng/d; ◆; $n = 6$), saline (■; $n = 12$), 1% Netrin-4 (2 ng/d; △; $n = 4$), or heat-denatured Netrin-4 (200 ng/d; ×; $n = 6$). (B) Thresholds at 24 h after administration were normalized to preadministration thresholds. (C) Immunofluorescence for c-fos in the L5 dorsal horn from the saline (left)- or Netrin-4 (right)–treated rats. The dashed lines represent the border between the gray and white matter in the lumbar cord. (D) The mean number of c-fos–expressing cells in 20-µm–thick hemisections from the L4-L5 dorsal horn. Data represent the mean from 4–6 rats. (E) Laminar distribution of c-fos–expressing cells in the superficial dorsal horn. (F) The mean number of c-fos–expressing cells in the L4-L5 dorsal horn of saline ($n = 3$)- or Netrin-4–administrated ($n = 7$) rats after brushing to the unilateral hind paw. Contra, contralateral. (G and H) Immunofluorescence of Iba1 (G) and GFAP (H) in saline- or Netrin-4–treated spinal cords. No obvious changes were noted in the morphology/cell number at 48 h after the administration of Netrin-4 (bottom) compared with the results from the saline-treated groups (top). (I) Paw withdrawal threshold after the administration of Netrin-4 (■; $n = 6$), minocycline with Netrin-4 (◇; $n = 6$), and L-a-aminoadipate (LAA) with Netrin-4 (○; $n = 4$). (J) Relative withdrawal thresholds at 24 h after administration. Bars: (C) 0.2 mm; (G and H) 50 µm. The data are presented as the mean ± SEM. *, $P < 0.05$; **, $P < 0.01$; ***, $P < 0.001$; ##, $P < 0.01$, versus saline-treated group; Tukey-Kramer test. Each experiment was performed three times in A–E and twice in F–J.

pain state. The antibody penetrated into lamina IIi or deeper and was bound to neuronal cells in the lumbar cord (Fig. 6, A and B) but not in the thoracic cord or in the cortex (not depicted). This analgesic effect lasted for at least 4 d after antibody administration (Fig. 6 C; 8 d after injury, $P < 0.05$; 9, 10, and 11 d after injury, $P < 0.01$ vs. the control IgG-treated

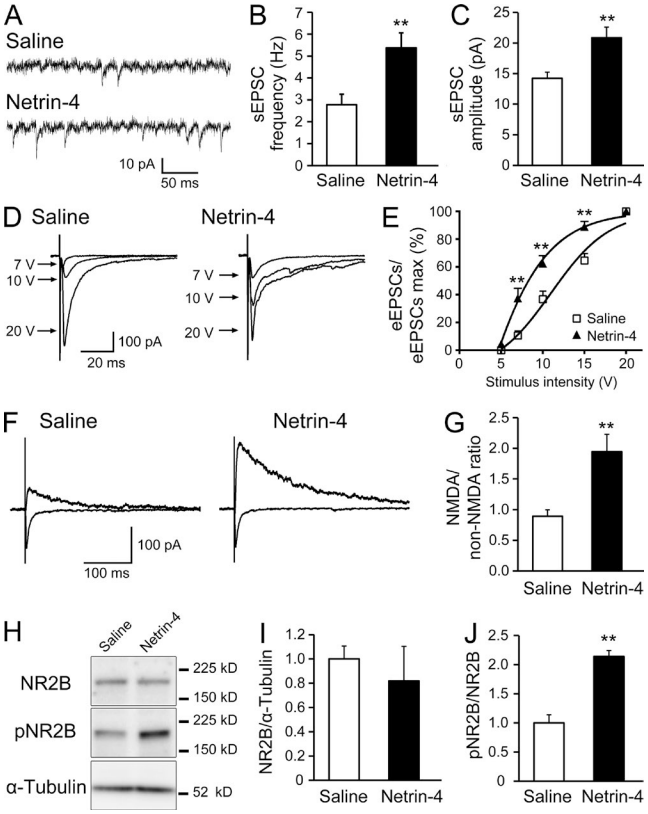

Figure 5. **Netrin-4 enhances excitatory synaptic transmission in the dorsal horn.** (A) Representative traces of sEPSCs recorded from dorsal horn lamina II neurons in spinal cord sections dissected from saline (top)- or Netrin-4 (bottom)–treated rats. The membrane potential was held at −60 mV in the presence of bicuculline and strychnine. Data represent the mean from 23 slices. (B and C) The frequency (B) and amplitude (C) of the sEPSCs were increased in the Netrin-4–treated group. Student's *t* test was used. (D) Representative traces of the eEPSCs recorded after stimulation of a neighboring area in the saline (left)- or Netrin-4 (right)–treated groups. (E) Leftward shift of the I-O curve of the eEPSCs in the Netrin-4–treated groups. Bonferroni test was used. (F) Representative traces of non-NMD AR–mediated eEPSCs at −60 mV (as indicated by the inward current) and NMDAR-mediated eEPSCs at 60 mV (as indicated by the outward current) in the saline (left)- or Netrin-4 (right)–treated groups. (G) Increase in the ratio of NMDAR/non-NMDAR–mediated components of the eEPSCs in the Netrin-4–treated group. Student's *t* test was used. (H) Western blot analysis of the dorsal spinal cord using antibodies against NR2B, phosphorylated NR2B (pNR2B), and α-tubulin. Data represent the mean from 5–6 rats. (I and J) Netrin-4 administration did not change NR2B expression (I) but increased pNR2B expression (J). Student's *t* test was used. The data are presented as the mean ± SEM. **, $P < 0.01$. Each experiment was performed three times in A–G and twice in H–J.

group). Lumbar spinal cord sections of PSL-injured rats were generated, and EPSCs from lamina II neurons in both the ipsilateral and contralateral sides were recorded to assess the electrophysiological properties of the dorsal horn circuits (Fig. 6, D–J). Compared with the contralateral side, the frequency of sEPSCs on the ipsilateral side was significantly increased (Fig. 6, D and E; $P < 0.05$; $n = 25$ for each group), as previously reported (Yan et al., 2013), although the amplitude of the sEPSCs was not altered (Fig. 6 F). This enhancement was abolished in the Netrin-4 antibody–treated PSL-injured rats ($P < 0.05$; $n = 24$ for each group).

To examine the synaptic responses of the dorsal horn neurons, eEPSCs were recorded by stimulating a neighboring area (Fig. 6, G and H). The I-O relationship was investigated by measuring the amplitude of the eEPSCs at each stimulus intensity. The I-O relation curve of the ipsilateral side of the PSL-injured rats exhibited a leftward shift compared with the contralateral side (Fig. 6 H; $P < 0.0001$; $n = 25$ for each group). At stimulus intensities of 7, 10, and 15 V, the synaptic responses on the ipsilateral side of the PSL-injured rats were significantly larger than those on the contralateral side (Fig. 6 H; $P < 0.05$ at 7 and 10 V; $P < 0.001$ at 15 V; $n = 25$ for each group). This leftward shift of the I-O relation curve was reversed by administration of the Netrin-4 antibody, as indicated by the significant shift of the I-O relation curve of the Netrin-4 antibody–treated PSL-injured rats compared with the control IgG-treated rats (Fig. 6 H; $P < 0.0001$; $n =$ 24–25 for each group). At stimulus intensities of 7, 10, and 15 V, the synaptic responses in Netrin-4 antibody–treated PSL-injured rats were significantly different than those in the control IgG-treated rats (Fig. 6 H; $P < 0.05$ at 7 and 10 V; $P <$ 0.001 at 15 V; $n = 24$–25 for each group). These data indicate that the evoked synaptic responses in the lamina II neurons were significantly enhanced on the ipsilateral side of the PSL-injured rats, whereas these responses were reversed by treatment with the Netrin-4 antibody.

Furthermore, the NMDA/non-NMDA ratio of the eEPSCs on the ipsilateral side of the PSL-injured rats was increased compared with the contralateral side, indicating an increase in NMDAR-mediated currents (Fig. 6 I; $P < 0.01$; $n =$ 25 for each group). This increase in the NMDA/non-NMDA ratio was abolished in the PSL-injured rats that were treated with the Netrin-4 antibody (Fig. 6, I and J; $P < 0.001$; $n =$ 24 for each group). Consistent with the present results, synaptic modulation in the dorsal horn circuit, such as increased presynaptic glutamate release (Yan et al., 2013) and increased NMDAR-mediated currents, contributes to neuropathic pain (Iwata et al., 2007; Yanagisawa et al., 2010; Cui et al., 2012; Yan et al., 2013). It is also known that the phosphorylation of the NR2B subunit of the NMDAR increases the open probability of the NMDAR leading to neuronal activation (Iwata et al., 2007). Collectively, these results show that endogenous Netrin-4 can enhance excitatory synaptic transmission by increasing glutamate release, synaptic responses, and NMD AR-mediated currents in the neuropathic pain state.

Unc5B mediates Netrin-4–induced and nerve injury–induced pain signaling

We next sought to identify functional receptors to which Netrin-4 binds to determine the molecular mechanisms underlying Netrin-4–induced tactile allodynia. Previous studies have shown that Netrin-4 binds to DCC, Neogenin, and

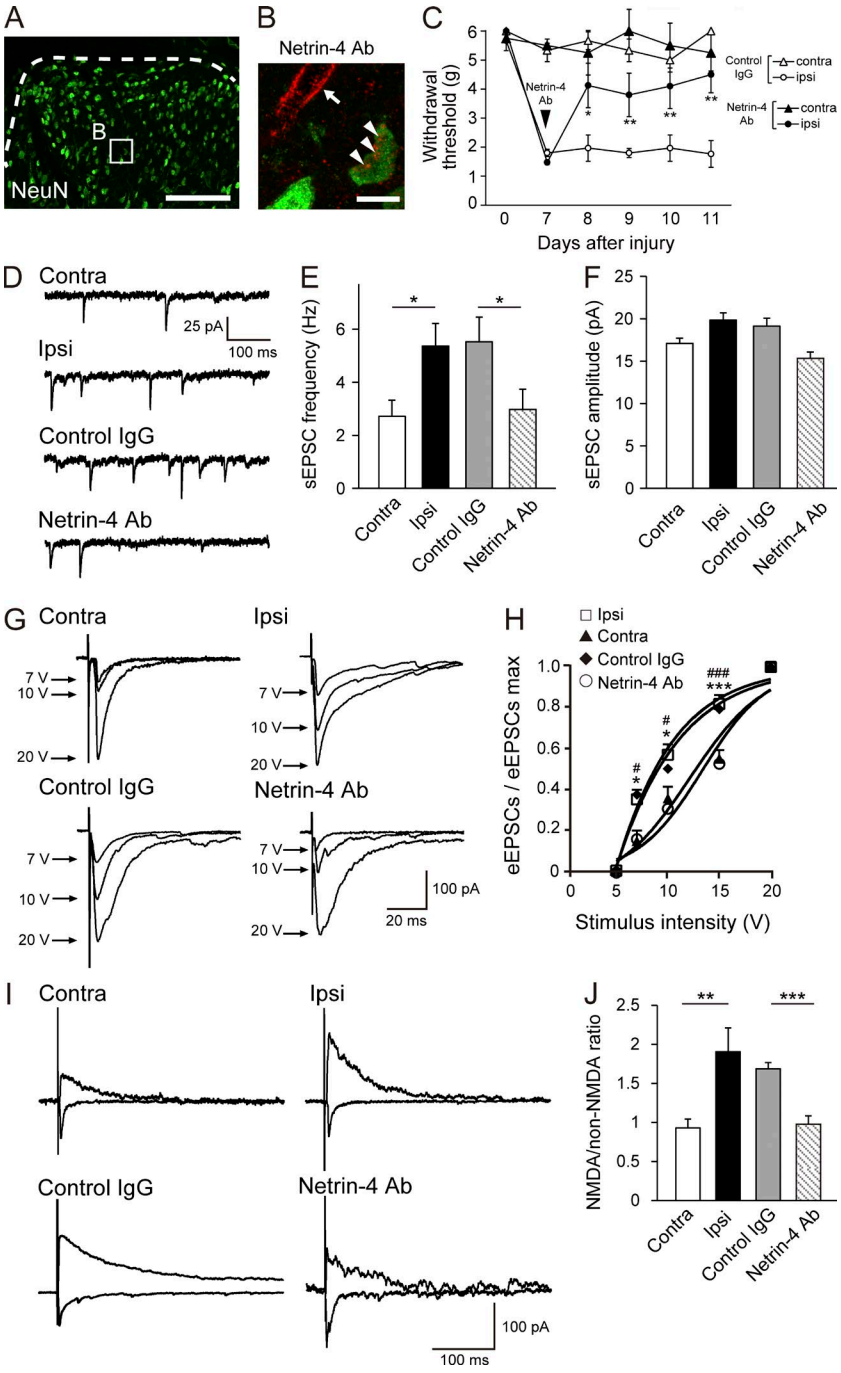

Figure 6. **The enhanced excitatory synaptic transmission in the model of neuropathic pain is abolished by a Netrin-4–blocking antibody.** (A and B) Penetration of the Netrin-4 antibody (Ab) into the dorsal horn. (B) Double immunofluorescence staining for the fluorescent dye–conjugated Netrin-4 antibody (HL-555; red) and NeuN (green). The fluorescence of the antibody was observed on neurons (arrowheads) and also around blood vessels (arrow) in lamina III (dashed lines in A). Bars: (A) 0.2 mm; (B) 10 µm. (C) Paw withdrawal of the control IgG (closed; $n = 11$)- or Netrin-4 antibody (open; $n = 11$)–treated animals after PSL injury. The data are presented as the mean ± SEM. *, $P < 0.05$; **, $P < 0.01$; Tukey-Kramer test. (D) Representative traces of the sEPSCs in the contralateral side, ipsilateral side, control IgG-treated, and Netrin-4 antibody–treated spinal cords. Electrophysiological data represent the mean from 25 slices. (E and F) The frequency (E) and amplitude (F) of the sEPSCs in each group. *, $P < 0.05$ vs. the contralateral side or control IgG-treated spinal cords; Student's t test. (G) Representative traces of the eEPSCs recorded after stimulation of a neighboring area. (H) The I-O curve of eEPSCs. *, $P < 0.05$; ***, $P < 0.001$ vs. the contralateral side. #, $P < 0.05$; ###, $P < 0.001$ vs. the control IgG-treated spinal cord; Bonferroni test. (I) Representative traces of non-NMDAR–mediated eEPSCs at −60 mV and NMDAR-mediated eEPSCs at 60 mV. (J) The ratio of NMDAR/non-NMDAR–mediated components of the eEPSCs in each group. **, $P < 0.01$ vs. the contralateral side; ***, $P < 0.001$ vs. the control IgG-treated spinal cord; Student's t test. The data are presented as the mean ± SEM. Each experiment was performed twice in A and B and three times in C–J. contra, contralateral; ipsi, ipsilateral.

Unc5A-D (Sun et al., 2011; Takemoto et al., 2011; Hayano et al., 2014). It has also been shown that Unc5B is strongly expressed in the adult dorsal spinal cord, whereas the other receptors are predominantly expressed in the ventral spinal cord (Manitt et al., 2004). Moreover, our immunohistochemical analysis showed that the Unc5B-positive (Unc5B$^+$) cells in the dorsal horn of the spinal cord (Fig. 7 A) and Unc5B$^+$ cells in the gray matter exclusively colocalized with the NeuN$^+$ cells (Fig. 7 B). In contrast, neither microglia nor astrocytes expressed Unc5B under pathological conditions (Fig. S4, A and B) and naive conditions (not depicted). These results are consistent with the observation that glial activation is independent of Netrin-4–induced allodynia (Fig. 4). We also examined the neuronal subtype of Unc5B$^+$ cells. Unc5B was expressed in some, but not all, of vGluT2$^+$, SOM$^+$, and Pax2$^+$ cells in the dorsal horn (Fig. S4, C–E), indicating broad expression of Unc5B in spinal cord neurons under pathological conditions and also under naive conditions (not depicted). Compared with the spinal cord, Unc5B gene expression levels in the DRG were <20% (Fig. S4 F).

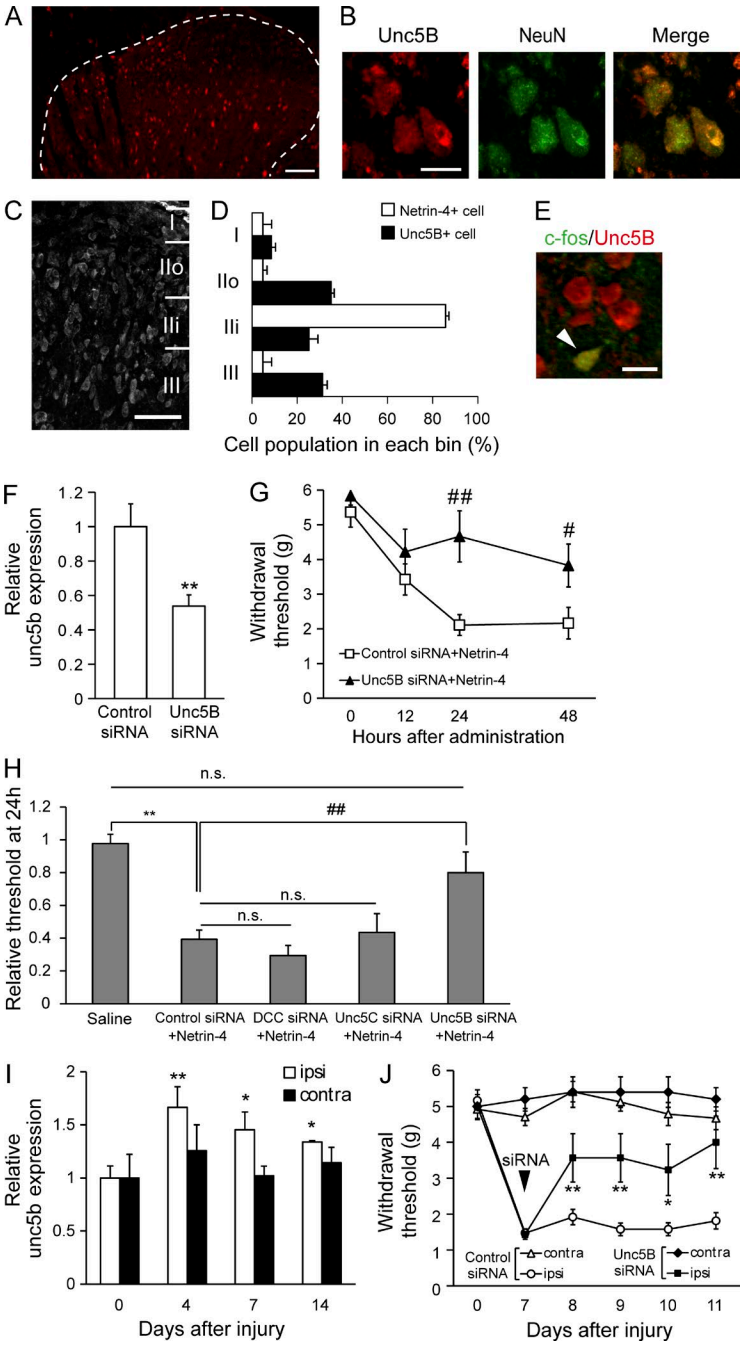

Figure 7. **The Unc5B receptor transduces Netrin-4–induced pain signaling.** (A) Unc5B immunofluorescence (red) in the dorsal horn of the spinal cord. (B) Unc5B and NeuN (green) double immunofluorescence. (C and D) Laminar distribution of Unc5B$^+$ cells in the superficial dorsal horn. (D) Comparison of the laminar distribution of Netrin-4 (unshaded) and Unc5B$^+$ cells (shaded). (E) Double immunofluorescence of Unc5B (red) and c-fos (green) in the Netrin-4–treated spinal cord. The arrowhead indicates colocalization of Unc5B and c-fos. (F) *Unc5b* mRNA expression at 4 d after siRNA administration. **, $P < 0.01$; Student's *t* test. (G) Paw withdrawals of the control siRNA (□; $n = 12$)– and Unc5B siRNA (▲; $n = 6$)–pretreated rats after Netrin-4 administration. #, $P < 0.05$; ##, $P < 0.01$; Tukey-Kramer test. (H) Relative withdrawal thresholds at 24 h after Netrin-4 administration. **, $P < 0.01$; ##, $P < 0.01$; Tukey-Kramer test. (I) *Unc5b* mRNA expression in the ipsilateral (ipsi; unshaded) and contralateral (contra; shaded) sides relative to the injury. *, $P < 0.05$; **, $P < 0.01$; Tukey-Kramer test. Data represent the mean from three to five rats. (J) Paw withdrawal of the control siRNA (open; $n = 12$)– or Unc5B siRNA (closed; $n = 10$)–treated rats after PSL injury. The siRNA was intrathecally administered 7 d after PSL injury. *, $P < 0.05$; **, $P < 0.01$; Tukey-Kramer test. Bars: (A) 0.1 mm; (B and E) 10 µm; (C) 50 µm. The data are presented as the mean ± SEM. Each experiment was performed twice in A–E and three times in F–J.

In contrast to the lamina-specific expression of Netrin-4 (Fig. 1, B and D), Unc5B$^+$ neurons were widely distributed in the superficial dorsal horn (Fig. 7, C and D). Moreover, most c-fos$^+$ cells in the Netrin-4–treated spinal cords expressed Unc5B (Fig. 7 E), supporting the notion that spinal Unc5B mediates Netrin-4–induced pain signaling. To test this, a siRNA directed against Unc5B was intraspinally transfected in vivo 2 d before Netrin-4 administration (Fig. 7, F and G). After Netrin-4 administration, the Unc5B siRNA–transfected rats ($n = 11$) showed an attenuation of the reduced paw withdrawal threshold compared with the control siRNA-transfected rats ($n = 13$; Fig. 7 G; 24 h, $P < 0.01$; 48 h, $P < 0.05$). At 24 h after transfection, the relative paw withdrawal threshold of Unc5B-siRNA–transfected rats was significantly increased to a level similar to the saline-treated rats ($n = 12$; Fig. 7 H; $P < 0.01$ vs. the control siRNA-treated group; $P > 0.05$ vs. the saline-treated group).

Gene expression of other Netrin receptors, such as DCC, Unc5A, or Unc5C, was not increased after peripheral nerve injury (Fig. S4, G–I). Further, the suppression of

DCC or Unc5C did not affect Netrin-4–induced allodynia (gene knock-down effect: 0.46 ± 0.11 for *dcc*; 0.29 ± 0.08 for *unc5c*; Fig. 7 H; $n = 6$ for DCC or Unc5C). These results indicated that Unc5B predominantly mediated Netrin-4–induced allodynia in the adult spinal cord. Moreover, a quantitative PCR analysis revealed that *unc5b* mRNA expression was significantly increased in the spinal cord ipsilateral to the injury after nerve injury (Fig. 7 I; 4 d after injury, $P < 0.05$; 7 and 14 d after injury, $P < 0.01$; $n = 4$ for each group), suggesting that Netrin-4–Unc5B signaling in the spinal cord could be enhanced after nerve injury. Importantly, intrathecal administration of Unc5B siRNA 7 d after PSL injury ($n = 10$) reversed the decrease in the paw withdrawal threshold (Fig. 7 J; 10 d after injury, $P < 0.05$; 8, 9, and 11 d after injury, $P < 0.01$, vs. the control siRNA-treated group). We further found that the Netrin-4 antibody, which suppressed tactile allodynia in the PSL model (Fig. 6), had the capacity to block direct binding between Netrin-4 and Unc5B (Fig. S4, J–L). Collectively, these results suggest that Unc5B was responsible for mediating Netrin-4–induced and nerve injury–induced allodynia.

SHP2 activation is required for Netrin-4–induced allodynia

We focused on SHP2, a protein tyrosine phosphatase containing Src homology 2 domains (Neel et al., 2003), to further explore the downstream mechanisms of Netrin-4–Unc5B signaling. Previous findings have shown that SHP2 binds to the intracellular domain of Unc5 and is activated by Netrin binding to Unc5 (Tong et al., 2001). Additionally, the phosphatase activity of SHP2 in the dorsal horn has been shown to be up-regulated after peripheral nerve injury (Peng et al., 2012). In the current study, we found that SHP2 protein was widely distributed throughout the dorsal horn of the spinal cord (Fig. 8 A), particularly in $Unc5B^+$ cells (Fig. 8 B). Moreover, intrathecal administration of Netrin-4 significantly increased the phosphatase activity of SHP2 in the dorsal spinal cord ($P < 0.05$ vs. saline; Fig. 8 C), whereas the addition of SHP2 inhibitors, NSC-87877, or PTPi IV attenuated phosphatase activity ($P < 0.01$ vs. the Netrin-4–treated group; Fig. 8 C; Peng et al., 2012). In addition, pretransfection of the Unc5B siRNA significantly blocked Netrin-4–induced SHP2 activation (Fig. 8 D; $P < 0.05$ vs. the control siRNA; $n = 4$ for each group). A previous study showed that PSL injury induced SHP2 activation in the injured side of the spinal cord, whereas the blockade of Netrin-4 function significantly reversed SHP2 activation (Fig. 8 E; $P < 0.01$; $n = 4$; Peng et al., 2012). These results suggest that Netrin-4 activates SHP2 by binding to Unc5B.

Moreover, we found that the SHP2 inhibitors NSC-87877 ($n = 6$) and PTPi IV ($n = 6$) could block the Netrin-4–induced decrease in the paw withdrawal threshold (Fig. 8, F and H; $P < 0.01$ vs. the Netrin-4–treated group). This change could also be observed by the increase in the relative withdrawal threshold values observed in the presence of the SHP2 inhibitors compared with those for the Netrin-4–treated group (Fig. 8 G; $n = 11$; $P < 0.01$); importantly, these values recovered to levels similar to those of the saline-treated groups ($n = 12$). Furthermore, intrathecal administration of PTPi IV ($n = 6$ for each group) significantly reversed the decrease in the withdrawal threshold after nerve injury (Fig. 8 H; $P < 0.01$ at 12 h and 24 h after administration vs. the saline-treated group). Western blot analysis revealed that NSC-87877 ($n = 4$) and PTPi IV ($n = 4$) significantly reduced Netrin-4–induced phosphorylation of NR2B in the spinal cord (Fig. 8, I–K; $P < 0.05$ vs. Netrin-4–treated group). Thus, SHP2 was involved in Netrin-4–induced synaptic modulation, presumably by acting downstream of Netrin-4–Unc5B, and the blockade of SHP2-attenuated neuropathic pain, which is consistent with a previous study (Peng et al., 2012).

DISCUSSION

Here, we identified a new molecular mechanism that contributes to neuropathic pain. Our results showed that Netrin-4, which is released from dorsal horn excitatory interneurons, enhanced excitatory synaptic transmission by phosphorylating NR2B, leading to neuronal activation in the dorsal horn and allodynia. Netrin-4–induced pain signaling was mediated by its binding to the Unc5B receptor and activation of the downstream intermediate SHP2. Peripheral nerve injury increased *unc5b* gene expression in the spinal cord, whereas expression of the *netrin-4* gene in the spinal cord or DRG was not altered (Fig. S5). Thus, injury-induced up-regulation of Unc5B expression in the dorsal horn may have accelerated neuronal excitation and induced hypersensitivity to sensory stimuli, causing tactile allodynia.

Our behavioral analysis revealed that Netrin-4 mutants did not exhibit tactile allodynia or heat hyperalgesia in the neuropathic pain model. Moreover, transient suppression of Netrin-4, the Unc5B receptor, or SHP2 prevented tactile allodynia at the second week after peripheral nerve injury. A similar abolishment of allodynia was also observed for inflammatory pain. Importantly, dorsal horn–specific expression of Netrin-4 was also observed in the spinal cord of multiple sclerosis patients (Khan and Smith, 2014). Therefore, the pain signal mediated by Netrin-4–Unc5B within the spinal cord may be relevant to humans. Thus, our current findings suggest that Netrin-4–Unc5B signaling may provide a promising molecular target for therapeutic strategies in pain relief.

After nerve injury or inflammation, the membrane excitability or synaptic efficacy of dorsal horn neurons is enhanced by various molecules derived from the surrounding cells (Latremoliere and Woolf, 2009; Milligan and Watkins, 2009). Injured primary afferents release neuropeptides, such as substance P, from the presynaptic terminal, which induce neuronal depolarization. Brain-derived neurotrophic factor (BDNF), a neurotrophin secreted from primary afferents or activated microglia, reduces the expression of the chloride transporter KCC2, causing the GABA receptors to switch

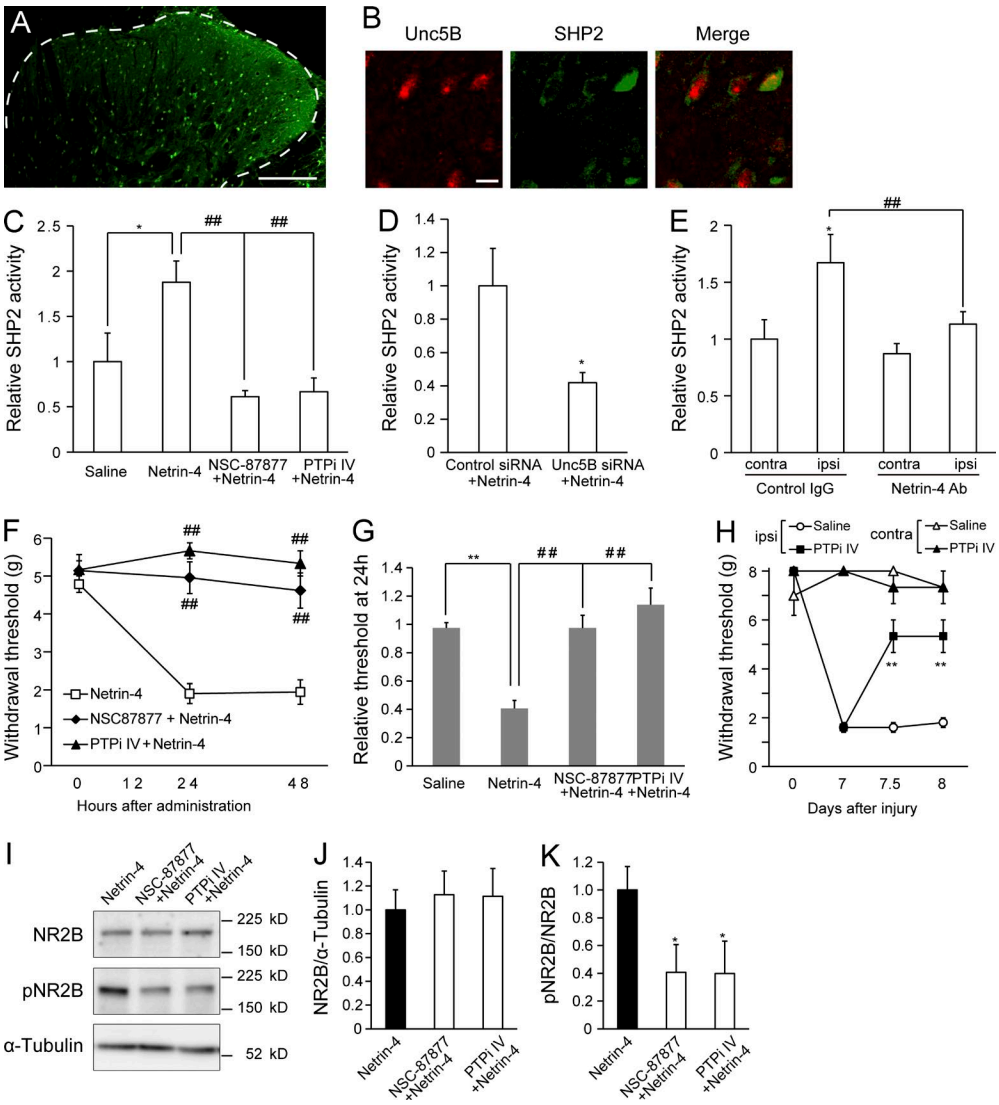

Figure 8. **SHP2 is crucial for mediating Netrin-4–induced tactile allodynia.** (A) SHP2 (green) immunofluorescence in the dorsal horn of the spinal cord. The dashed line indicates the border between white and gray matter. (B) Double-immunofluorescence labeling for SHP2 and Unc5B (red). Bars: (A) 0.2 mm; (B) 10 µm. (C) SHP2 phosphatase activity at 48 h after saline ($n = 6$), Netrin-4 ($n = 5$), NSC87877 plus Netrin-4 ($n = 5$), and PTPi IV plus Netrin-4 administration. *, $P < 0.05$; ##, $P < 0.01$; Tukey-Kramer test. (D) SHP2 phosphatase activity in the control siRNA– or Unc5B siRNA–pretreated dorsal spinal cords at 48 h after Netrin-4 administration. *, $P < 0.05$; Student's t test. (E) SHP2 phosphatase activity in the contralateral (contra) and ipsilateral (ipsi) sides relative to the injury in the control IgG- or Netrin-4 antibody (Ab)–treated spinal cords ($n = 6$ for each group). *, $P < 0.05$; ##, $P < 0.01$; Tukey-Kramer test. (F) Paw withdrawal after intrathecal administration of Netrin-4 (□; $n = 5$), NSC-87877 plus Netrin-4 (◆; $n = 6$), and PTPi IV plus Netrin-4 (▲; $n = 4$). ##, $P < 0.01$; Tukey-Kramer test. (G) The relative thresholds at 24 h after administration were normalized to the preadministration thresholds. **, $P < 0.01$; ##, $P < 0.01$; Tukey-Kramer test. (H) Paw withdrawal of the control saline (open; $n = 6$)- or PTPi IV (closed; $n = 6$)–treated animals after PSL injury. The data are presented as the mean ± SEM. **, $P < 0.01$; Tukey-Kramer test. (I) Western blot analysis of dorsal spinal cord tissues using antibodies against NR2B, phosphorylated NR2B (pNR2B), and α-tubulin. (J and K) The NSC-87877 and PTPi IV treatments did not change NR2B expression (J) but decreased the pNR2B/NR2B ratio compared with the Netrin-4–treated group (K). *, $P < 0.05$; Dunnett's test. Data represent the mean from four to seven rats. The data are presented as the mean ± SEM. Each experiment was performed twice in A and B and three times in C–K.

from inhibitory to excitatory signaling (Tsuda et al., 2003; Pezet and McMahon, 2006). Activated microglia- or astrocyte-derived cytokines or chemokines increase the excitability of dorsal horn projection neurons (Calvo et al., 2012). Furthermore, 5-HT release from the descending fibers of the rostral ventromedial medulla facilitates the excitation of dorsal horn neurons (Porreca et al., 2002). It is notable that Netrin-4 is distinct from these previously identified pain-inducing molecules, as Netrin-4 is secreted from locally innervating dorsal horn interneurons to modify the pain circuit (Morris

et al., 2004; Todd, 2010). Pathological conditions frequently alter the properties of interneurons by reducing GABA/glycine release or the development of potentiation, leading to central sensitization (Baron, 2006; Sandkühler, 2009). Our present findings provide a new perspective, as local molecular signals derived from dorsal horn interneurons might lead to hyperexcitability in the dorsal horn and hypersensitivity in neuropathic pain. Therefore, this distinctive feature (i.e., a new ligand–receptor interaction and the downstream pathway) might make a significant impact on the development of effective treatments.

Our histochemical analysis shows that the Netrin-4–expressing neurons are excitatory neurons (Fig. 1 F and Fig. S1, A–D), and their nuclei are located exclusively in lamina IIi (Fig. 1, B–D; and Fig. S1, E–G). Collectively with previous studies showing the classification of lamina II interneurons based on their dendritic morphology (Todd, 2010), our findings suggest that Netrin-4 is secreted from excitatory interneurons such as vertical cells, radial cells, and central cells. Recent studies have reported the importance of excitatory interneurons in pain processing both in physiological and pathological conditions (Duan et al., 2014; Peirs et al., 2015). Because electrophysiological recordings revealed Netrin-4 enhanced excitatory synaptic transmission in lamina II (Figs. 5 and 6), these results suggest that the Netrin-4 secreted from excitatory interneurons in lamina IIi may increase the excitability of lamina II neurons, such as vertical, radial, and central cells (Zheng et al., 2010; Zeilhofer et al., 2012). Thus, our present findings provide a new mechanism for how a specific population of interneurons induces spinal sensitization, leading to chronic pain. Furthermore, we identify Netrin-4 as a new marker of a subset of excitatory interneurons. Therefore, our findings contribute to future studies aimed at elucidating the precise function and molecular identity of excitatory interneurons and their critical role in pain signaling (Prescott et al., 2014).

Our electrophysiological results showed that spinal Netrin-4 increased both the sEPSCs and eEPSCs of dorsal horn neurons. The increase in NMDAR-mediated eEPSCs in the Netrin-4–treated spinal cord could be dependent on the phosphorylation of NR2B. After peripheral nerve injury, SHP2 activation in the dorsal horn increases binding between PSD-95 and NR2B, and this binding enhances the phosphorylation of NR2B, leading to the development of neuropathic pain (Peng et al., 2012). Thus, the Netrin-4–Unc5B–SHP2 signaling pathway might enhance postsynaptic NMDAR signaling in the dorsal horn, which could contribute to neuropathic pain (Lin et al., 1999).

Together with the observation that NR2B phosphorylation is crucial to the development and maintenance of inflammatory pain (Guo et al., 2002), our results raise the possibility that Netrin-4 might regulate signaling that is common to both neuropathic and inflammatory pain. Another possible mechanism is that Netrin-4 elicits two different pain-signaling pathways induced by nerve injury or inflammation. It has been reported that an increased amplitude of sEPSCs was observed in inflammatory pain but not in neuropathic pain (Iwata et al., 2007; Yan et al., 2013). Our current results showed that the sEPSC amplitudes recorded from the dorsal horn neurons were increased by Netrin-4 administration, although the Netrin-4–blocking antibody did not alter this effect after PSL injury (Fig. 5 C and Fig. 6 F). This result suggested that Netrin-4 function, which increased the amplitude of sEPSCs, was not activated in the neuropathic state. Thus, further investigations of Netrin-4 function in other pain models could be important for obtaining a better understanding of the differences between different types of pain. Moreover, Netrin is known to promote axonal growth and branching in the nervous systems during development (Manitt et al., 2009; Hayano et al., 2014). Therefore, it is also possible that Netrin-4 alters neuronal wiring in the dorsal horn after nerve injury (Woolf and Salter, 2000).

The present study showed that Netrin-4 regulates synaptic modulation and central sensitization, leading to neuropathic pain. Our current findings revealed that in addition to its canonical role in development, Netrin also plays an important role in the adult nervous system and in certain pathological conditions. Together with the observation that Netrins and their receptors are expressed in the adult nervous system (Ellezam et al., 2001), our present findings suggest the possibility that Netrin proteins may be involved in a broader array of neural functions than previously expected.

MATERIALS AND METHODS

Animals

8–10-wk-old male Wistar/ST rats (200–280 g; Japan SLC) were used in the current study. All experiments, with the exception of electrophysiological assessment, were conducted in accordance with the Osaka University Medical School Guide for the Care and Use of Laboratory Animals and were approved by the Institutional Committee of Osaka University. Preparation of animals for electrophysiological assessment and patch clamp assay were conducted in accordance with the Association for Assessment and Accreditation of Laboratory Animal Care (AAALAC) international guidelines for the care and use of laboratory animals; the protocol was approved by the Shionogi Research Laboratories Institutional Animal Care and Use Committee (IACUC).

Pain models

PSL was performed as has been previously described (Seltzer et al., 1990). In brief, rats were put under isoflurane anesthesia, and PSL was produced by tying a tight ligature around the diameter of the sciatic nerve located on the left, ipsilateral side. The nerve on the right, contralateral side was left exposed without ligation. Inflammatory pain was then modeled under anesthesia by subcutaneously injecting 20 µl of 50% CFA (Sigma-Aldrich) into the left hind paw (Newbould, 1963).

Behavioral tests

The mechanical sensitivity of animals was assessed using the von Frey filament test, as previously described (Chaplan et al., 1994). Rats were individually placed in a plastic cage on wire mesh and habituated for 5–10 min. Calibrated von Frey filaments (Semmes-Weinstein von Frey esthesiometer; Muromachi Kikai) were applied to the plantar surface of the rat hind paw from below the mesh wire, and a 50% withdrawal threshold was determined using the up-down method. Thermal nociception was then assessed with an infrared source as the latency to withdrawal from a radiant heat stimulus using a plantar test device (model 7370; Ugo Basile). All behavioral analyses were done under a single-blind condition.

Catheter implantation

For intrathecal administration, a modified version of the catheter-through-a-needle technique was applied based on a previous study (Maeda et al., 2009). Under 2% isoflurane, a catheter of polyethylene tubing (PE-10; Clay-Adams; BD) was inserted between lumbar vertebrae L5 and L6. To verify catheter placement, lidocaine was injected, followed by saline; hind paw paralysis indicated successful catheterization. Animals showing neurological deficits after catheter implantation were excluded from subsequent drug/protein administration or behavioral tests.

siRNA administration

siRNA against Netrin-4 or Unc5B was purchased from Invitrogen (Stealth RNAi siRNA Select RNAi; in vivo purity). The off-target effect of each siRNA was validated in vitro; after transfection of siRNA to RNB cells, gene expression of other Netrin family or the appropriate receptor family members was examined using the quantitative PCR technique. Furthermore, we confirmed the rescue of the gene knock-down effect by cotransfection of the siRNA-resistant form of each gene. The siRNA that showed no off-target effect was used in this study. For in vivo gene knock-down, siRNAs with transfection reagents (HVJ Envelope Vector kit GenomeONE Neo; Ishihara Sangyo) were administered according to the manufacturer's instructions. In brief, after 250 µl HVJ-E vector (five assay units) was mixed with 25 µl of the enclosing factor, the mixture was centrifuged, and the pellet was suspended in 100 µl of saline. A mixture of Netrin-4 or Unc5B siRNAs (1, 2, and 3; 1 µg/µl each) was added, and the solution was kept on ice for 5 min. 10 µl of the siRNA solution was then injected once per experiment through the catheter into the subarachnoid space, followed by flushing with 10 µl of saline. As a control, the same volume of control siRNA (Stealth RNAi siRNA Negative Control Med GC; Invitrogen) in an HVJE solution was used. To confirm the incorporation of siRNA into spinal cord neurons, 10 µg of fluorescent dye HiLyte Fluor488-conjugated control siRNA (Nippon Gene) was intrathecally administered via an implanted catheter. 2 d after siRNA administration, spinal cord tissue was dissected out and fixed for immunohistochemistry.

Intrathecal administration of drugs and recombinant proteins

Mouse Netrin-4 recombinant protein (1132-N4; R&D Systems) was diluted using saline. The Netrin-4 mixture was then boiled for 10 min to denature the protein. To suppress glial cell or SHP2 activity, 40 µg/µl minocycline (M9511; Sigma-Aldrich), 30 nmol/µl L-a-aminoadipate (A0637; Sigma-Aldrich), 1 mM SHP inhibitor 8-hydroxy-7-(6-sulfonaphthalen-2-yl) diazenyl-quinoline-5-sulfonic acid (NSC-87877; 56932; EMD Millipore) or 1 mM SHP2 inhibitor PTP inhibitor IV (PTPi4; 540211; EMD Millipore) was mixed with the Netrin-4 protein just before intrathecal injection. Less than 2% isoflurane, 10 µl of protein, or drug-containing solution was slowly injected into the catheterized tubing, followed by the tubing being fitted to a saline-filled micro-osmotic pump (0.25 µl per hour; model 1002; Alzet). The pump was subcutaneously inserted into the back of the rats, which enabled sustained administration of drug or protein for at least 48 h. In Fig. 4 F, 1 d after Netrin-4 administration, 3 min of low-threshold mechanical stimulation was applied to the left hind paw with a paintbrush, followed by sacrifice. A mouse anti–Netrin-4 antibody (AF1132; R&D Systems) or control rat IgG (I8015; Sigma-Aldrich) was diluted to 1 µg/µl with saline and intrathecally injected into the catheterized tubing (30 µg), followed by flushing with 10 µl of saline.

Genotyping of Netrin-4–mutant rats

Genotyping for Netrin-4–mutant rats was performed using PCR amplification with the following primers: 5′-TCC CGGTTCTTGCTAAGCAGAGG-3′ and 5′-TGGTGC ACGAGCACGAACTAGG-3′ for the wild-type allele and 5′-CTTGTGTCATGCACAAAGTAGATGTCC-3′ and 5′-TGGTGCACGAGCACGAACTAGG-3′ for the mutant allele. After denaturation at 95°C for 5 min, the mixture was incubated for 35 cycles of 1 min each at 95, 55, and 72°C, followed by a 7-min extension at 72°C.

Immunohistochemistry

Rats were deeply anaesthetized by intraperitoneal injection of 100 mg/kg pentobarbital and were then transcardially perfused with 50 ml PBS, followed by 150 ml of ice-cold 4% paraformaldehyde in a 0.1 M phosphate buffer (PB). The fourth to sixth lumbar segments of the spinal cord were dissected out and postfixed in the same fixative for 6 h at 4°C. Segments were then transferred from fixative to 30% sucrose in PBS for 48 h at 4°C. 20-µm coronal spinal cord cryosections were obtained, washed three times, and incubated in blocking solution (5% fetal bovine serum albumin and 0.3% Triton X) for 2 h at room temperature (RT). Then, sections were incubated for either 24 or 48 h at 4°C with the following primary antibodies: Netrin-4 (1:50; HPA049832), Unc5B (1:200; HPA01141; ATLAS), NeuN (1:1,000; ABN91; EMD Millipore), Iba1 (1:500; 019-19741; Wako Pure Chemical Industries), CD11b (1:500; 550299; BD), GFAP (1:400; G-A-5; Sigma-Aldrich), SHP2 (1:1,000; sc-280; Santa Cruz

Biotechnology, Inc.), c-fos (1:2,000; Ab-5; EMD Millipore), serine racemase (1:100; 612052; BD), SOM (1:100; MAB354; EMD Millipore), vGluT2 (1:2,000; AB5907; EMD Millipore), or LacZ (1:2,000; 559761; Cappel). Sections were washed three times and incubated overnight at 4°C in a secondary antibody solution (Alexa Fluor 488 and/or 546; 1:500; Molecular Probes). The next day, tissue sections were washed, slide mounted, and subsequently cover slipped with mounting media using the cellular nuclear marker DAPI (Vector Laboratories). We obtained autopsied spinal cord tissues from an individual with relapsing-remitting multiple sclerosis and used the autopsied spinal cord section from an individual with polymyositis as a control. The research protocol was approved by the Human Use Review Committees of the Graduate School of Medicine, Chiba University for the Protection of Human Subjects. The paraffin sections were deparaffinized with Clear Plus and then rehydrated in a descending ethanol series. The sections were treated in the blocking solution of 0.1 M PB, pH 7.4, containing 0.3% Triton X, 2% BSA (Sigma-Aldrich), and 5% normal donkey serum (Gibco) for 1 h at RT and then rinsed with 0.1 M PB. The sections were then incubated for 2 h at RT and then two overnights at 4°C with a polyclonal goat anti–Netrin-4 (1:100; AF1254; R&D Systems) primary antibody in blocking solution. After washing extensively with 0.1 M PB, the sections were incubated with the biotin-conjugated donkey anti–goat IgG secondary antibody (1:200; Vector Laboratories) for 2 h at RT in PB with 3% BSA. Thereafter, the sections were treated in 1% H_2O_2 for 30 min at RT to eliminate endogenous peroxidases. After amplification with avidin–biotin complex (ABC kit; Vector Laboratories), the reaction product was visualized with 50 mM Tris-buffered saline (TBS), pH 7.4, including 2.5% 3,3′-diaminobenzidine (DAB), 0.04% $NiCl_2$, and 0.75% H_2O_2. The reaction was stopped by immersion in 50 mM TBS followed by dehydration. Finally, the sections were sealed with Entellan medium (Merck).

X-gal staining

The spinal cord was fixed with 4% paraformaldehyde in a 0.1 M PB for 3–4 h, followed by cryoprotection with 15 and 30% sucrose in PBS. Then, frozen tissues were cut into 50-µm coronal sections with a cryostat; after two washes with PBS containing 2 mM $MgCl_2$, the sections were incubated with a staining solution (1 mg/ml X-gal, 5 mM potassium ferricyanide crystalline, 5 mM potassium ferricyanide trihydrate, and 2 mM $MgCl_2$ in 0.01 M PB with saline) at 37°C overnight. After X-gal staining, immunohistochemistry was further performed to examine the identity of $LacZ^+$ cells. To block endogenous peroxidase activity, sections were incubated in 0.3% H_2O_2 containing 70% methanol at RT for 30 min. After incubation with 5% normal goat serum in 0.3% Triton X/PBS, sections were incubated with the following primary antibodies and concentrations: biotin-conjugated IB4 (1:200; L 2140; Sigma-Aldrich), vGluT1 (1:1,000; 135 304; Synaptic Systems), calcitonin gene-related peptide (1:200; CA1134; Enzo Life Sciences), Pax2 (1:500; 71-6000; Invitrogen), serine racemase (1:100; 612052; BD), and parvalbumin (1:1,000; PVG-214; Swant). Sections were washed three times and incubated overnight at 4°C in secondary antibody solutions (biotin-conjugated rabbit/mouse/goat/guinea pig IgG, respectively; Vector Laboratories). After incubation with ABC reagent (Vector Laboratories) at RT for 30 min, sections were placed in a peroxidase substrate solution until stain intensity developed. Stained sections were then mounted onto glass slides, dehydrated, and cover-slipped with Eukitt.

Spinal cord slice preparation for electrophysiological studies

8-wk-old male Wistar/ST rats (Japan SLC) weighing 230–280 g were used for electrophysiological studies. The rats were housed in a vivarium with a 12-h alternating light-dark cycle and were given food and water ad libitum. Electrophysiological experiments were conducted in accordance with the AAALAC guidelines for the care and use of laboratory animals; the protocol was approved by the Shionogi Research Laboratories IACUC. The rats were anesthetized with 3% isoflurane, and 40 ng/10 µl Netrin-4 protein solution (R&D Systems) was directly injected between lumbar vertebrae L4 and L5 using a 25-Ga needle attached to a Hamilton microsyringe. Intrathecal injection of Netrin-4 protein or saline solution was performed twice daily for 2 d. After injection, the rats were individually placed in a heated cage until recovery from anesthesia. The withdrawal threshold was measured by the up-down method of a von Frey monofilament stimulation to the plantar surface of each hind paw. Mechanical sensitivity was shown in the mean of the withdrawal threshold of each hind paw. 24–48 h after intrathecal administration, rats were decapitated under 60 mg/kg i.p. sodium pentobarbital anesthesia. The spinal cords were isolated and placed in ice-cold, low-sodium artificial cerebrospinal fluid (CSF) containing the following: 100 mM choline chloride, 13 mM NaCl, 3 mM KCl, 1 mM NaH_2PO_4, 25 mM $NaHCO_3$, 11 mM D-glucose, 1 mM $CaCl_2$, and 5 mM $MgCl_2$, pH 7.4, after bubbling with 95% O_2 and 5% CO_2. 300-µm transverse slices were prepared using a vibratome (VT1200S; Leica Biosystems) and maintained for at least 60 min in standard artificial CSF containing the following: 113 mM NaCl, 3 mM KCl, 1 mM NaH_2PO_4, 25 mM $NaHCO_3$, 11 mM D-glucose, 2 mM $CaCl_2$, and 1 mM $MgCl_2$, pH 7.4, after bubbling with 95% O_2 and 5% CO_2. Slices were transferred to a recording chamber mounted on the stage of a microscope (BX51-WI; Olympus) and superfused with standard artificial CSF (flow rate of 2.5 ml/min at 30–32°C).

Patch-clamp recordings of excitatory synaptic currents

Whole-cell voltage-clamp recordings were made from visually identified substantia gelatinosa neurons using an upright microscope (BX51WI; Olympus) with infrared differential interference contrast optics. Patch electrodes (2.5–3-µm tip diameter) were pulled from borosilicate glass capillaries and had resistance of 3–5 MΩ when filled with an internal

solution consisting of the following: 140 mM CsCl, 10 mM Hepes, 1.1 mM EGTA, 2 mM $MgCl_2$, 3 mM MgATP, 5 mM QX-314, and 0.3 mM Tris–guanosine triphosphate, pH 7.4 (adjusted with CsOH). EPSCs were detected as inward deflections (EPC-10; HEKA), low-pass filtered at 2.9 kHz, and digitized at 10 kHz for computer analysis with Pulse software (HEKA) and Chart 5 (ADInstruments). Access resistance was monitored using measuring capacitive transients obtained in response to a hyperpolarizing voltage step (10 mV for 10 ms) from a holding potential of −60 mV. All experiments were performed at 30–32°C. We investigated changes in excitatory synaptic transmission among spinal slices using the following three parameters. (1) Frequency and amplitude of sEPSCs: sEPSCs were recorded in the presence of 10 μM bicuculline and 3 μM strychnine to block GABAergic and glycinergic inhibitory synaptic transmission, respectively. sEPSCs recorded at a holding potential of −60 mV were mediated by non-NMDARs. The frequency and amplitude of sEPSC events were analyzed with the Mini Analysis Program (Synaptosoft Inc.). Changes in the frequency and amplitude of sEPSCs reflect presynaptic changes in glutamate release probability and postsynaptic changes, such as the function of a glutamate receptor, respectively. In the current experiment, we examined the mean frequency and amplitude of sEPSCs for 2 min. (2) I-O relation curve of eEPSCs: eEPSCs were induced by stimulating the neighboring area (within a 40–100-μm radius of the recorded neuron) via a glass pipette filled with 1 M NaCl solution. eEPSCs recorded at a holding potential of −60 mV were mediated by a non-NMDAR. A voltage pulse 0.2 ms in duration was gradually increased from a threshold to a maximal response value (5–20 V). An I-O relation curve was constructed by plotting the relative amplitude of eEPSCs to the maximal amplitude at each stimulus intensity. The curve shift was evaluated to check the effect of Netrin-4 protein or Netrin-4 antibody. (3) Ratio of NMDAR-mediated eEPSCs to non-NMDAR–mediated eEPSCs: We compared the ratio of NMDAR-mediated eEPSCs to non-NMDAR–mediated eEPSCs between experimental groups. After non-NMDAR–mediated eEPSCs were recorded after electrical stimulation at suprathreshold intensity (1.5× the threshold), NMDAR-mediated eEPSCs were induced at a holding potential of 60 mV in the presence of a non-NMDAR blocker CNQX (10 μM), after electrical stimulation at the same intensity.

Western blot analysis

Rats were deeply anaesthetized and transcardially perfused with 100 ml of PBS. The dorsal side of spinal cords at L4–L6 were dissected out, lysed using a mixture containing 50 mM Tris-HCl, pH 7.4, 150 mM NaCl, 1% NP-40, 0.1% SDS, and a protease inhibitor cocktail (Complete; 11697498001; Roche) and phosphatase inhibitor (PhosSTOP; 04906837001; Roche). The homogenate was centrifuged at 8,000 *g* for 10 min, and the supernatant was used for the following experiments. Tissue lysates were boiled in a sample buffer for 5 min, and proteins were separated using SDS-polyacrylamide gel (6% acrylamide) electrophoresis and transferred onto polyvinylidene difluoride membranes (EMD Millipore). The membranes were blocked with 5% BSA in a TBS/0.1% Tween 20 (TBST) buffer and incubated for 1 h at RT. They were then incubated overnight at 4°C with anti-NR2B (1:500; TA309191; OriGene), anti-phosphorylated (Tyr1472) NR2B (1:500; TA309196; OriGene), or an anti–α-tubulin antibody (1:1,000; sc-5286; Santa Cruz Biotechnology, Inc.) in TBST buffer containing 1% BSA. After washing in TBST, the membrane was incubated with horseradish peroxidase–conjugated anti–rabbit IgG antibody (Cell Signaling Technology) or anti–mouse IgG antibody (Cell Signaling Technology) for 1 h at RT. Signals were detected with an enhanced chemiluminescence system (GE Healthcare) using an image analyzer (LAS-3000; Fujifilm). The band intensity was quantified using ImageJ software (National Institutes of Health).

Quantitative PCR

Total RNA was extracted from the fourth and fifth lumbar spinal cord segments with TRIzol reagent (Invitrogen). After cDNA synthesis (High-capacity cDNA RT kit; Roche), gene expression was quantified with a TaqMan Gene Expression Assay (Applied Biosystems). Rat glyceraldehyde-3-phosphate dehydrogenase was used as an endogenous control to normalize gene expression (4352338E; Applied Biosystems). To amplify sequences of specific genes of interest, the following primer pairs and a universal probe were used: for Netrin-4, 5′-CCCATGTACTGGCGGAGA-3′ and 5′-GCGGAGGTTGGTGATCTTC-3′ (Universal Probe Library no. 68); for unc5b, 5′-CCCATGTACTGGCGGAGA-3′ and 5′-GCGGAGGTTGGTGATCTTC-3′ (Universal Probe Library no. 76); for unc5a, 5′-GACACCCGCAACTGTACCA-3′ and 5′-CCGATGTAGAGAGCCACGTC-3′ (Universal Probe Library no. 13); for unc5c, 5′-CCACCGTCATCGTGTATGTT-3′ and 5′-GGCTGTTACACACAGACCATTC-3′ (Universal Probe Library no. 83); and for dcc, 5′-CTGTCTGTGGACCGAGGTTT-3′ and 5′-TTGTGCTGTTGGTCCTTCAC-3′ (Universal Probe Library no. 15). The resulting cycle threshold (Ct) values were calculated by the ΔCt method to obtain fold-differences.

Measurement of SHP2 phosphatase activity

Phosphatase activity of SHP2 was measured using the Active SHP2 DuoSet IC kit (R&D Systems) according to the manual provided. Under than 2% isoflurane, the dorsal parts of the fourth and fifth lumbar spinal cord segments were dissected out, homogenized in lysis buffer, and centrifuged; subsequently, the supernatant of the sample was removed. SHP-2 immunoprecipitation agarose beads were mixed with each sample and incubated at 4°C for 3 h. After rinsing with a 1-mM dithiothreitol-containing buffer, tyrosine phosphatase substrate was added to the samples, which were then incubated at 37°C for 30 min. After brief centrifugation, the supernatant was transferred to a 96-well plate, and malachite green coloring reagent was added to each well. After incu-

bation at RT, the absorbance of each sample was measured at 620 nm on a microplate reader (Molecular Devices). The measured concentrations for each well were then subtracted from those of sodium orthovanadate–containing control wells. Finally, concentrations of phosphate were normalized using the protein concentration of each sample.

Statistical analyses

Statistical analyses were performed using Student's *t* test for comparison between two groups and two-way analysis of variance with posthoc Tukey-Kramer tests for multiple groups. Differences were considered significant at $P < 0.05$. All data are represented as mean ± SEM.

Online supplemental material

Fig. S1 shows neuronal subtype and localization of Netrin-4–expressing cells in the dorsal horn. Fig. S2 demonstrates Netrin-4 expression in nociceptive pathways. Fig. S3 explains the procedure for the electrophysiological analyses after Netrin-4 administration. Fig. S4 indicates that spinal cord neurons express Unc5B, which acts as a Netrin-4 receptor. Fig. S5 shows Netrin-4 expression after peripheral nerve injury.

ACKNOWLEDGMENTS

We thank A. Kawabata, M. Tsubota-Matsunami, T. Okubo, and S. Ohnami for their expert technical assistance. We also thank T. Yasaka for helpful and important suggestions.

This work was supported by a Grant-in-Aid for Scientific Research (S) from the Japan Society for the Promotion of Science (25221309).

The authors declare no competing financial interests.

Author contributions: Y. Hayano, K. Takasu, K. Ogawa, and T. Yamashita designed research. Y. Hayano performed all of the experiments, with the exception of the portions indicated below. K. Minami prepared animals for electrophysiological experiments, K. Takasu performed whole-cell patch recording of each spinal cord slice, and K. Minami contributed to the preparation of Netrin-4 transgenic animals. S. Kuwabara provided human subjects, and Y. Koyama and M. Yamada performed immunohistochemistry. Y. Hayano and K. Takasu analyzed data. Y. Hayano, K. Takasu, K. Ogawa, K. Minami, T. Asaki, and T. Yamashita drafted the manuscript. T. Yamashita coordinated and directed the project.

Submitted: 8 June 2016
Revised: 1 September 2016
Accepted: 24 October 2016

REFERENCES

Antal, M., E. Polgár, J. Chalmers, J.B. Minson, I. Llewellyn-Smith, C.W. Heizmann, and P. Somogyi. 1991. Different populations of parvalbumin- and calbindin-D28k-immunoreactive neurons contain GABA and accumulate ^{3}H-D-aspartate in the dorsal horn of the rat spinal cord. *J. Comp. Neurol.* 314:114–124. http://dx.doi.org/10.1002/cne.903140111

Baron, R. 2006. Mechanisms of disease: neuropathic pain—a clinical perspective. *Nat. Clin. Pract. Neurol.* 2:95–106. http://dx.doi.org/10.1038/ncpneuro0113

Baron, R., A. Binder, and G. Wasner. 2010. Neuropathic pain: diagnosis, pathophysiological mechanisms, and treatment. *Lancet Neurol.* 9:807–819. http://dx.doi.org/10.1016/S1474-4422(10)70143-5

Calvo, M., J.M. Dawes, and D.L.H. Bennett. 2012. The role of the immune system in the generation of neuropathic pain. *Lancet Neurol.* 11:629–642. http://dx.doi.org/10.1016/S1474-4422(12)70134-5

Chaplan, S.R., F.W. Bach, J.W. Pogrel, J.M. Chung, and T.L. Yaksh. 1994. Quantitative assessment of tactile allodynia in the rat paw. *J. Neurosci. Methods.* 53:55–63. http://dx.doi.org/10.1016/0165-0270(94)90144-9

Cheng, L., A. Arata, R. Mizuguchi, Y. Qian, A. Karunaratne, P.A. Gray, S. Arata, S. Shirasawa, M. Bouchard, P. Luo, et al. 2004. Tlx3 and Tlx1 are post-mitotic selector genes determining glutamatergic over GABAergic cell fates. *Nat. Neurosci.* 7:510–517. http://dx.doi.org/10.1038/nn1221

Cirulli, V., and M. Yebra. 2007. Netrins: beyond the brain. *Nat. Rev. Mol. Cell Biol.* 8:296–306. http://dx.doi.org/10.1038/nrm2142

Costigan, M., J. Scholz, and C.J. Woolf. 2009. Neuropathic pain: a maladaptive response of the nervous system to damage. *Annu. Rev. Neurosci.* 32:1–32. http://dx.doi.org/10.1146/annurev.neuro.051508.135531

Cui, G.B., J.Z. An, N. Zhang, M.G. Zhao, S.B. Liu, and J. Yi. 2012. Elevated interleukin-8 enhances prefrontal synaptic transmission in mice with persistent inflammatory pain. *Mol. Pain.* 8:11. http://dx.doi.org/10.1186/1744-8069-8-11

Duan, B., L. Cheng, S. Bourane, O. Britz, C. Padilla, L. Garcia-Campmany, M. Krashes, W. Knowlton, T. Velasquez, X. Ren, et al. 2014. Identification of spinal circuits transmitting and gating mechanical pain. *Cell.* 159:1417–1432. http://dx.doi.org/10.1016/j.cell.2014.11.003

Ellezam, B., I. Selles-Navarro, C. Manitt, T.E. Kennedy, and L. McKerracher. 2001. Expression of netrin-1 and its receptors DCC and UNC-5H2 after axotomy and during regeneration of adult rat retinal ganglion cells. *Exp. Neurol.* 168:105–115. http://dx.doi.org/10.1006/exnr.2000.7589

Guo, H., and L.-Y.M. Huang. 2001. Alteration in the voltage dependence of NMDA receptor channels in rat dorsal horn neurones following peripheral inflammation. *J. Physiol.* 537:115–123. http://dx.doi.org/10.1111/j.1469-7793.2001.0115k.x

Guo, W., S. Zou, Y. Guan, T. Ikeda, M. Tal, R. Dubner, and K. Ren. 2002. Tyrosine phosphorylation of the NR2B subunit of the NMDA receptor in the spinal cord during the development and maintenance of inflammatory hyperalgesia. *J. Neurosci.* 22:6208–6217.

Hargreaves, K., R. Dubner, F. Brown, C. Flores, and J. Joris. 1988. A new and sensitive method for measuring thermal nociception in cutaneous hyperalgesia. *Pain.* 32:77–88. http://dx.doi.org/10.1016/0304-3959(88)90026-7

Hayano, Y., K. Sasaki, N. Ohmura, M. Takemoto, Y. Maeda, T. Yamashita, Y. Hata, K. Kitada, and N. Yamamoto. 2014. Netrin-4 regulates thalamocortical axon branching in an activity-dependent fashion. *Proc. Natl. Acad. Sci. USA.* 111:15226–15231. http://dx.doi.org/10.1073/pnas.1402095111

Iwata, H., T. Takasusuki, S. Yamaguchi, and Y. Hori. 2007. NMDA receptor 2B subunit-mediated synaptic transmission in the superficial dorsal horn of peripheral nerve-injured neuropathic mice. *Brain Res.* 1135:92–101. http://dx.doi.org/10.1016/j.brainres.2006.12.014

Ji, X.-T., N.-S. Qian, T. Zhang, J.-M. Li, X.-K. Li, P. Wang, D.-S. Zhao, G. Huang, L. Zhang, Z. Fei, et al. 2013. Spinal astrocytic activation contributes to mechanical allodynia in a rat chemotherapy-induced neuropathic pain model. *PLoS One.* 8:e60733. http://dx.doi.org/10.1371/journal.pone.0060733

Kennedy, M.B., and P. Manzerra. 2001. Telling tails. *Proc. Natl. Acad. Sci. USA.* 98:12323–12324. http://dx.doi.org/10.1073/pnas.231486398

Kennedy, T.E., T. Serafini, J.R. de la Torre, and M. Tessier-Lavigne. 1994. Netrins are diffusible chemotropic factors for commissural axons in the embryonic spinal cord. *Cell.* 78:425–435. http://dx.doi.org/10.1016/0092-8674(94)90421-9

Khan, N., and M.T. Smith. 2014. Multiple sclerosis-induced neuropathic pain: pharmacological management and pathophysiological insights from rodent EAE models. *Inflammopharmacology.* 22:1–22. http://dx.doi.org/10.1007/s10787-013-0195-3

Kitada, K., S. Ishishita, K. Tosaka, R. Takahashi, M. Ueda, V.W. Keng, K. Horie, and J. Takeda. 2007. Transposon-tagged mutagenesis in the rat. *Nat. Methods.* 4:131–133. http://dx.doi.org/10.1038/nmeth1002

Koch, M., J.R. Murrell, D.D. Hunter, P.F. Olson, W. Jin, D.R. Keene, W.J. Brunken, and R.E. Burgeson. 2000. A novel member of the netrin family, β-netrin, shares homology with the β chain of laminin: identification, expression, and functional characterization. *J. Cell Biol.* 151:221–234. http://dx.doi.org/10.1083/jcb.151.2.221

Latremoliere, A., and C.J. Woolf. 2009. Central sensitization: a generator of pain hypersensitivity by central neural plasticity. *J. Pain.* 10:895–926. http://dx.doi.org/10.1016/j.jpain.2009.06.012

Lesnick, T.G., S. Papapetropoulos, D.C. Mash, J. Ffrench-Mullen, L. Shehadeh, M. de Andrade, J.R. Henley, W.A. Rocca, J.E. Ahlskog, and D.M. Maraganore. 2007. A genomic pathway approach to a complex disease: axon guidance and Parkinson disease. *PLoS Genet.* 3:e98. http://dx.doi.org/10.1371/journal.pgen.0030098

Lin, S.Y., K. Wu, G.W. Len, J.L. Xu, E.S. Levine, P.C. Suen, H.T. Mount, and I.B. Black. 1999. Brain-derived neurotrophic factor enhances association of protein tyrosine phosphatase PTP1D with the NMDA receptor subunit NR2B in the cortical postsynaptic density. *Brain Res. Mol. Brain Res.* 70:18–25. http://dx.doi.org/10.1016/S0169-328X(99)00122-9

Maeda, Y., Y. Aoki, F. Sekiguchi, M. Matsunami, T. Takahashi, H. Nishikawa, and A. Kawabata. 2009. Hyperalgesia induced by spinal and peripheral hydrogen sulfide: evidence for involvement of Cav3.2 T-type calcium channels. *Pain.* 142:127–132. http://dx.doi.org/10.1016/j.pain.2008.12.021

Manitt, C., K.M. Thompson, and T.E. Kennedy. 2004. Developmental shift in expression of netrin receptors in the rat spinal cord: predominance of UNC-5 homologues in adulthood. *J. Neurosci. Res.* 77:690–700. http://dx.doi.org/10.1002/jnr.20199

Manitt, C., A.M. Nikolakopoulou, D.R. Almario, S.A. Nguyen, and S. Cohen-Cory. 2009. Netrin participates in the development of retinotectal synaptic connectivity by modulating axon arborization and synapse formation in the developing brain. *J. Neurosci.* 29:11065–11077. http://dx.doi.org/10.1523/JNEUROSCI.0947-09.2009

Maraganore, D.M., M. de Andrade, T.G. Lesnick, K.J. Strain, M.J. Farrer, W.A. Rocca, P.V.K. Pant, K.A. Frazer, D.R. Cox, and D.G. Ballinger. 2005. High-resolution whole-genome association study of Parkinson disease. *Am. J. Hum. Genet.* 77:685–693. http://dx.doi.org/10.1086/496902

Milligan, E.D., and L.R. Watkins. 2009. Pathological and protective roles of glia in chronic pain. *Nat. Rev. Neurosci.* 10:23–36. http://dx.doi.org/10.1038/nrn2533

Morris, R., O. Cheunsuang, A. Stewart, and D. Maxwell. 2004. Spinal dorsal horn neurone targets for nociceptive primary afferents: do single neurone morphological characteristics suggest how nociceptive information is processed at the spinal level. *Brain Res. Brain Res. Rev.* 46:173–190. http://dx.doi.org/10.1016/j.brainresrev.2004.07.002

Nakashiba, T., T. Ikeda, S. Nishimura, K. Tashiro, T. Honjo, J.G. Culotti, and S. Itohara. 2000. Netrin-G1: a novel glycosyl phosphatidylinositol-linked mammalian netrin that is functionally divergent from classical netrins. *J. Neurosci.* 20:6540–6550.

Neel, B.G., H. Gu, and L. Pao. 2003. The 'Shp'ing news: SH2 domain-containing tyrosine phosphatases in cell signaling. *Trends Biochem. Sci.* 28:284–293. http://dx.doi.org/10.1016/S0968-0004(03)00091-4

Newbould, B.B. 1963. Chemotherapy of arthritis induced in rats by mycobacterial adjuvant. *Br. Pharmacol. Chemother.* 21:127–136. http://dx.doi.org/10.1111/j.1476-5381.1963.tb01508.x

Peirs, C., S.P. Williams, X. Zhao, C.E. Walsh, J.Y. Gedeon, N.E. Cagle, A.C. Goldring, H. Hioki, Z. Liu, P.S. Marell, and R.P. Seal. 2015. Dorsal horn circuits for persistent mechanical pain. *Neuron.* 87:797–812. http://dx.doi.org/10.1016/j.neuron.2015.07.029

Peng, H.-Y., G.-D. Chen, C.-Y. Lai, M.-C. Hsieh, and T.-B. Lin. 2012. Spinal SIRPα1-SHP2 interaction regulates spinal nerve ligation-induced neuropathic pain via PSD-95-dependent NR2B activation in rats. *Pain.* 153:1042–1053. http://dx.doi.org/10.1016/j.pain.2012.02.006

Petrenko, A.B., T. Yamakura, H. Baba, and K. Shimoji. 2003. The role of N-methyl-D-aspartate (NMDA) receptors in pain: a review. *Anesth. Analg.* 97:1108–1116. http://dx.doi.org/10.1213/01.ANE.0000081061.12235.55

Pezet, S., and S.B. McMahon. 2006. Neurotrophins: mediators and modulators of pain. *Annu. Rev. Neurosci.* 29:507–538. http://dx.doi.org/10.1146/annurev.neuro.29.051605.112929

Porreca, F., M.H. Ossipov, and G.F. Gebhart. 2002. Chronic pain and medullary descending facilitation. *Trends Neurosci.* 25:319–325. http://dx.doi.org/10.1016/S0166-2236(02)02157-4

Prescott, S.A., Q. Ma, and Y. De Koninck. 2014. Normal and abnormal coding of somatosensory stimuli causing pain. *Nat. Neurosci.* 17:183–191. http://dx.doi.org/10.1038/nn.3629

Sandkühler, J. 2009. Models and mechanisms of hyperalgesia and allodynia. *Physiol. Rev.* 89:707–758. http://dx.doi.org/10.1152/physrev.00025.2008

Schwarting, G.A., D. Raitcheva, E.P. Bless, S.L. Ackerman, and S. Tobet. 2004. Netrin 1-mediated chemoattraction regulates the migratory pathway of LHRH neurons. *Eur. J. Neurosci.* 19:11–20. http://dx.doi.org/10.1111/j.1460-9568.2004.03094.x

Seltzer, Z., R. Dubner, and Y. Shir. 1990. A novel behavioral model of neuropathic pain disorders produced in rats by partial sciatic nerve injury. *Pain.* 43:205–218. http://dx.doi.org/10.1016/0304-3959(90)91074-S

Srour, M., J.-B. Rivière, J.M.T. Pham, M.-P. Dubé, S. Girard, S. Morin, P.A. Dion, G. Asselin, D. Rochefort, P. Hince, et al. 2010. Mutations in DCC cause congenital mirror movements. *Science.* 328:592. http://dx.doi.org/10.1126/science.1186463

Sun, K.L.W., J.P. Correia, and T.E. Kennedy. 2011. Netrins: versatile extracellular cues with diverse functions. *Development.* 138:2153–2169. http://dx.doi.org/10.1242/dev.044529

Tabata-Imai, A., R. Inoue, and H. Mori. 2014. Increased sensitivity to inflammatory pain induced by subcutaneous formalin injection in serine racemase knock-out mice. *PLoS One.* 9:e105282. http://dx.doi.org/10.1371/journal.pone.0105282

Takahashi, T., Y. Aoki, K. Okubo, Y. Maeda, F. Sekiguchi, K. Mitani, H. Nishikawa, and A. Kawabata. 2010. Upregulation of Cav3.2 T-type calcium channels targeted by endogenous hydrogen sulfide contributes to maintenance of neuropathic pain. *Pain.* 150:183–191. http://dx.doi.org/10.1016/j.pain.2010.04.022

Takemoto, M., Y. Hattori, H. Zhao, H. Sato, A. Tamada, S. Sasaki, K. Nakajima, and N. Yamamoto. 2011. Laminar and areal expression of unc5d and its role in cortical cell survival. *Cereb. Cortex.* 21:1925–1934. http://dx.doi.org/10.1093/cercor/bhq265

Todd, A.J. 2010. Neuronal circuitry for pain processing in the dorsal horn. *Nat. Rev. Neurosci.* 11:823–836. http://dx.doi.org/10.1038/nrn2947

Tong, J., M. Killeen, R. Steven, K.L. Binns, J. Culotti, and T. Pawson. 2001. Netrin stimulates tyrosine phosphorylation of the UNC-5 family of netrin receptors and induces Shp2 binding to the RCM cytodomain. *J. Biol. Chem.* 276:40917–40925. http://dx.doi.org/10.1074/jbc.M103872200

Tsuda, M., Y. Shigemoto-Mogami, S. Koizumi, A. Mizokoshi, S. Kohsaka, M.W. Salter, and K. Inoue. 2003. $P2X_4$ receptors induced in spinal microglia gate tactile allodynia after nerve injury. *Nature.* 424:778–783. http://dx.doi.org/10.1038/nature01786

Woolf, C.J., and M.W. Salter. 2000. Neuronal plasticity: increasing the gain in pain. *Science.* 288:1765–1768. http://dx.doi.org/10.1126/science.288.5472.1765

Yan, X., E. Jiang, M. Gao, and H.-R. Weng. 2013. Endogenous activation of presynaptic NMDA receptors enhances glutamate release from the

primary afferents in the spinal dorsal horn in a rat model of neuropathic pain. *J. Physiol.* 591:2001–2019. http://dx.doi.org/10.1113/jphysiol.2012.250522

Yanagisawa, Y., H. Furue, T. Kawamata, D. Uta, J. Yamamoto, S. Furuse, T. Katafuchi, K. Imoto, Y. Iwamoto, and M. Yoshimura. 2010. Bone cancer induces a unique central sensitization through synaptic changes in a wide area of the spinal cord. *Mol. Pain.* 6:38. http://dx.doi.org/10.1186/1744-8069-6-38

Yasaka, T., S.Y.X. Tiong, D.I. Hughes, J.S. Riddell, and A.J. Todd. 2010. Populations of inhibitory and excitatory interneurons in lamina II of the adult rat spinal dorsal horn revealed by a combined electrophysiological and anatomical approach. *Pain.* 151:475–488. http://dx.doi.org/10.1016/j.pain.2010.08.008

Zeilhofer, H.U., H. Wildner, and G.E. Yévenes. 2012. Fast synaptic inhibition in spinal sensory processing and pain control. *Physiol. Rev.* 92:193–235. http://dx.doi.org/10.1152/physrev.00043.2010

Zheng, J., Y. Lu, and E.R. Perl. 2010. Inhibitory neurones of the spinal substantia gelatinosa mediate interaction of signals from primary afferents. *J. Physiol.* 588:2065–2075. http://dx.doi.org/10.1113/jphysiol.2010.188052